NOVEL APPROACHES TO ULTRAFAST FIBER LASER DESIGN FOR ABLATION-COOLED MATERIAL REMOVAL

A DISSERTATION SUBMITTED TO
THE GRADUATE SCHOOL OF ENGINEERING AND SCIENCE
OF BILKENT UNIVERSITY
IN PARTIAL FULFILLMENT OF THE REQUIREMENTS FOR
THE DEGREE OF
DOCTOR OF PHILOSOPHY
IN
PHYSICS

By
Saniye Sinem YILMAZ
September 2016

Novel approaches to ultrafast fiber laser design for ablation-cooled material removal

By Saniye Sinem YILMAZ

September 2016

We certify that we have read this dissertation and that in our opinion it is fully adequate, in scope and in quality, as a dissertation for the degree of Doctor of Philosophy.

Fatih Ömer İlday(Advisor)

Coşkun Kocabaş

Uwe Morgner

Ömer Morgül

Alphan Sennaroğlu

Approved for the Graduate School of Engineering and Science:

Ezhan Karaşan
Director of the Graduate School

ABSTRACT

NOVEL APPROACHES TO ULTRAFAST FIBER LASER DESIGN FOR ABLATION-COOLED MATERIAL REMOVAL

Saniye Sinem YILMAZ
Ph.D. in Physics
Advisor: Fatih Ömer İlday
September 2016

The past few decades in particular have witnessed the tremendous beneficial impact of innovations in laser technology ranging from biomedical to industrial applications in response to enhancing community's quality of life. From the beginning, laser technology, especially ultrafast lasers have provided a very convenient platform for producing need-based laser signals, which are addressed to a wide variety of scientific and technological problems. However, there is a scarcity of utilization of ultrafast lasers as well-developed tools for various applications, mostly in industry and research laboratories due to their complexity, low reliability and high cost as a result of the dominance of solid-state lasers. Fiber lasers, on the other hand, are inherently inexpensive, compact in size and robust in their operation under harsh conditions.

Applications of ultrafast laser material processing have become extremely diverse, yet ultrafast material processing is still extremely complex, costly and quite slow in terms of material removal, which is particularly taxing for biological tissue removal, rendering ultrafast lasers uncompetitive compared to mechanical techniques. This thesis represents a series of work about developing fiber laser systems which address this technological problem. The motivation of this thesis is to develop fiber laser systems for applying the ablation cooled laser material removal idea which has recently proposed by our group [1] for tissue and material processing. Ablation cooling becomes significant above a certain repetition rate, which depends on the thermal diffusivity of the target material. Besides, the speed with which the laser beam can be repositioned over a target is limited. As a remedy, burst-mode operation, also proposed by our group [2] has been implemented, where the laser produces groups of high repetition rate pulses, which are, in turn, repeated with a lower frequency. Consequently, the burst-mode fiber laser system operating at 1 μm was demonstrated with an all-fiber architecture and we scaled it to 100 MHz intra-burst repetition rate and 1 MHz burst repetition rate

with the average power of 150 W for high power applications. Additionally, a detailed investigation on the limits of continuously-pumped all-fiber burst mode laser system was reported.

Besides all the practical advantages of the ablation cooling idea compared to other laser-material interactions, laser ablation depends on laser operating wavelength because materials have wavelength dependent absorption and scattering values. In terms of underlying laser technology, ultrafast tissue ablation experiments require a laser system operating around 2 μm where laser tissue interaction is much stronger due to the local peak of water absorption for achieving a high ablation efficiency. Therefore, this thesis also focuses on transferring know-how on burst-mode operation to the Tm/Ho doped fiber system, operating around 2 μm, which addresses requirements for an efficient tissue ablation process without any collateral damage. The physics of the laser-material interaction assisted by ablation cooling idea is also valid for tissue ablation, so the repetition rates of several GHz are necessary for fully exploiting this effect. Toward this goal, we developed core technologies, which were constituted by three different stages: (i) starting from a novel mode-locked oscillator with a repetition rate in the GHz range, (ii) followed by the construction of a Tm-doped pump source based on the WDM cascade architecture and (iii) finally the amplification of the Ho-doped fiber with a dual wavelength pumping concept.

Keywords: Fiber lasers, Ytterbium doped fibers, Thulium doped fibers, Holmium doped fibers, burst-mode operation, all-fiber structure, WDM cascade, the spectral beam combination, high repetition rate oscillators.

ÖZET

SOĞUK ABLASYONLU MALZEME KALDIRMA UYGULAMALARI İÇİN ULTRAHIZLI FİBER LAZER TASARIMINA YENİ YAKLAŞIMLAR

Saniye Sinem YILMAZ
Fizik, Doktora
Tez Danışmanı: Fatih Ömer İlday
Eylül 2016

Lazer teknolojisi, geçtiğimiz son on yılda, insan ihtiyaçlarina bağlı olarak çok büyük atılımlar göstermiş olup, uygulama alanları biyomedikalden endüstriyel uygulamalara kadar genişlemiştir. Özellikle ultra-hızlı lazerlerin, ihtiyaç duyulan uygulama alanına göre farklı özelliklerde sinyal üretebilmeleri bir çok bilimsel ve teknolojik problemlerin de çözülmesine olanak sağlamıstır. Ancak, endüstriyel ve bilimsel olarak bakıldığında bir çok araştırma ve geliştirme laboratuvarlarında, bu tarz lazerlerin kullanımında hala bir kısıtlama görülmektedir. Bu durumun sebebi ise yüksek fiyatlı, düşük güvenirliliğe sahip; yapısal ve kullanım olarak karmaşık olan katı-hal lazerlerinin bu alandaki egemenliği olarak kabul edilebilir. Öteki taraftan fiber lazerler katı-hal lazerlerine oranla, fiberin yapısından kaynaklı olarak daha ucuz, boyut olarak kompakt ve zor şartlar altında daha dayanıklı bir platform sağlamaktadırlar.

Ultra-kısa atımların kullanılması, lazerle mikro-imalat alanında önemli gelişmelere yol açmıştır. Yine de bu sistemler ile yapilan malzeme işleme uygulamaları diğer mekanik yöntemlere kıyasla; karmaşık lazer yapıları, yavaş operasyon süreleri ve yüksek maaliyetleri yüzünden özellikle biyolojik doku üzerindeki işlemler gibi bir çok malzeme işlemleri icin çok fazla tercih edilmemektedirler. Bunlara bağlı olarak, bu tez daha verimli malzeme kaldırma rejiminin uygulanabilmesi için fiber lazer sistemlerinin geliştirilmesi hakkında yapılan calışmaları içermektedir. Amacımız, gurubumuzun keşfi olan ablasyon soğutmalı lazerle malzeme kaldırma (ablation-cooled material removal) fikrini doku [1] ve malzeme işlemede uygulama imkanını yaratacak ve hem endüstriyel olarak mikro-imalat alanında hem de lazer cerrahisine yönelik büyük potansiyel taşıyan bir ultrakısa atımlı lazer sistemleri elde etmektir. Ablasyon soğumasından faydalanabilmek için tekrar frekansının belli bir eşiği geçmesi gerekmektedir. Bu eşik ise malzemenin ısı iletkenliği ile doğru orantılıdır. Bununla beraber, artan tekrar

frekansı, lazer ışınının malzeme üzerinde ilerlemesini sağlayan elektronik cihazların hızı tarafından limitlenmektedir. Kendi gurubumuz tarafından geliştirilen [2], hedeflenen sıklıkta ve enerjideki atımları düşük frekansta tekrarlanan kümeler içinde sağlayan küme-modlu lazer teknolojisi, malzeme işleme uygulamalarında karşılaşılan bu problemler için çözüm olabilir. Bu sebepler doğrultusunda, küme modlu ve yüksek güçlü bir fiber sistemi gelişitirildi, tasarlandı ve kuruldu. Yükselteç, 1 μm dalga boyunda ışıyan 100 MHz tekrar frekanslı, kip kilitli fiber salıngaç tarafından beslenmektedir. Bu fiber lazer sistemi, 150 W ortalama güce kadar küme modunda atımlar yaratabilmektedir ve sistemdeki ortalama atım enerjisi 14.5 μJ olup, tekrar frekansı 1 MHzdir. Ayrıca sürekli pompalanan, fiberle tümleşik küme modlu lazer sisteminin, limitlerinin detaylı incelenmeside bu tez kapsamında gösterilmiştir.

Ablasyon soğutmali lazerle malzeme kaldırma fikrinin diğer lazer-malzeme etkileşimlerine kıyasla bir çok avantajı olmasına rağmen; malzeme işleme verimi lazerin dalga boyuna bağlı olarak çok büyük bir artış gösterir. Geliştirilmesi gereken lazer teknolojisi açısından bakıldığında, ultra-hızlı doku ablasyon deneyleri icin 2 μm dalga boyunda ışıyan lazerler gerekmektedir, çünkü dokularda yüksek miktarda bulunan suyun lokal soğurma tepesinin 1.94 mikronda olması, aynı serbest çalışma dalga boyunda ısıyan lazerler ile, ablasyon soğutmalı rejimin doku kaldırmada etkisinin çok daha ileri boyutlara taşınacağını öngörülebilir. Bu tezde, ablasyon soğutmalı lazer ile malzeme kaldırma deneylerimiz için geliştirmiş olduğumuz 1 mikron dalga boyunda çalışan İterbiyum (Yb) fiber tabanlı küme-modlu tümleşik fiber lazer teknolojisini, doku ile etkileşimin çok daha yüksek olduğu 2 mikron dalga boyuna taşımayı hedefliyoruz. Ablasyon soğutmalı lazerle malzeme kaldırma işleminin altında yatan fizik doku da dahil olmak üzere bütün malzemeler için geçerli olup, ancak tam olarak etkinin gözlemlenmesi için bu frekansın GHz mertebelerine ulaşması gerekmektedir. Bu amaçla, tezin bu kısmında doku işleme amaçlı kullanılacak lazer sistemi için gerekli olan ana parcaları geliştirdik. Bu amaçla ilk olarak (i) GHz tekrar frekansına sahip kip-kilitli fiber lazer salingacı tasarlanılmış ve inşa edilmiştir. Buna muteakiben sırası ile (ii) pompa kaynağı olarak kullanılmak amaçlı; kademeli olarak tasarlanan WDM şeması esas alınarak, yüksek güçlü, fiberle tümleşik sürekli dalga Tm katkılı fiber lazer sisteminin geliştirilmesi; son olarak (iii) Ho katkılı fiber yükseltecinin kurulup, iki farklı dalga boyunda ışıyan fiber lazerle pompalanması gösterilmiştir.

Anahtar sözcükler: Fiber lazerler, İterbiyum katkılı fiberler, Tulyum katkılı fiberler, Holmiyum katkılı fiberler, küme-modlu operasyon, fiberle tümleşik

yapı, WDM kademeli yapı, spektral ışın kombinasyonu, yüksek tekrar frekanslı salıngaçlar .

Acknowledgement

During my time as a student at the Bilkent University, I had a great time, I also admit that it was a long, tiresome and emotional process. Nevertheless, I really enjoyed every moment of this time that I spent and I have gained much experience both on a theoretical, technical and personal level. I could not have finished without the emotional and intellectual support that I get. Therefore, there are many people that I would like to acknowledge for this time.

I am deeply indebted to my supervisor F. Ömer İlday for giving me the possibility of working with such an interesting field as fiber lasers and his fundamental role in my life. He provided me with every bit of guidance, assistance and expertise that I needed during my the process that I underwent in undergraduate and graduate school. Ömer gave me the freedom to do whatever I wanted, at the same time continuing to contribute valuable feedback, advice and encouragement. Furthermore, he helped me to learn how to become an individual scientist and stubbornly overcome the problems. I quite simply cannot imagine a better supervisor.

I am very thankful to Hakan Sayınç for his kindest support, motivation and guidance in every possible way, where he made this possible and being a good friend ever since.

I gratefully acknowledge the members of my Ph.D. committee members for their time and valuable feedback about my works.

I would like to thank to Hamit Kalaycıoğlu and Parviz Elahi for their close collaboration at various stages of my thesis.

During my study, I would like to thank Ihor Pavlov and Emrah İlbey for their friendships, supports and fruitful scientific discussions.

I would especially like to thank Kutan Gürel, Denizhan Kesim, Özgün Yavuz and Uğur Teğin for their collaborations and the great times that we shared.

I am grateful to Seydi Yavaş, Önder Akcaalan, Bülent Öktem, Onur Tokel, Ahmet Turnali, Gizem Gencoğlu and all other current and former members of UFOLAB for being helpful and friendly to me.

I am deeply thankful to Emre Ozan Polat for making all boring days shiny.

I would like to thank Cem Sipahi for his infinite patience, understanding and support.

I thank to my parents Ömür & Kenan and my beloved brother Serkan Yılmaz for their love, understanding and for always being *there*.

Ozymandias

I met a traveller from an antique land
Who said: Two vast and trunkless legs of stone
Stand in the desert . . . Near them, on the sand,
Half sunk, a shattered visage lies, whose frown,
And wrinkled lip, and sneer of cold command,
Tell that its sculptor well those passions read
Which yet survive, stamped on these lifeless things,
The hand that mocked them, and the heart that fed:
And on the pedestal these words appear:
My name is Ozymandias, king of kings:
Look on my works, ye Mighty, and despair!'
Nothing beside remains. Round the decay
Of that colossal wreck, boundless and bare
The lone and level sands stretch far away.

Percy Bysshe Shelley

Dedicated to my family

Contents

List of Figures

List of Tables

Chapter 1

Introduction

1.1 Motivation

The field of laser development has a relatively short history since the invention of the first laser by Maiman at 1960 [5]. Nevertheless, after the first demonstration, it has gained a rapidly growing interest in the way we communicate, in the practice of medicine and in the tools we use to explore the frontiers of science which could not be imagined just a few decades ago. The explosive developments and applications in different studies of the laser science has blossomed with the utilization of sources of ultrashort light pulses. After this scientific impact, the main advances in laser technology were done in two directions; shorter pulses and higher peak powers [6] and in order to achieve this purpose, many laser types have been developed [7–11]. Although the laser field is pervasive in modern life, it has a role as a technological enabler which is essential but generally plays a supporting role in a larger system. Therefore, compact, easy to operate and low costs systems will be required if ultrashort lasers are expanding their application areas at the outside of research laboratories in the biology facilities, industrial applications for manufacturing, medical clinics and even in cosmatic facilities and aircrafts. To this date, the dominant platform for the ultrafast lasers is based on solid state technology. Despite tremendous commercially-motivated effort, these

systems are still prohibitively complicated, expensive and unreliable for many applications outside of the research laboratory. Laser sources that are significantly more compact, more robust, and inexpensive can have a major impact on the dissemination of ultrafast optics applications. In the past 20 years, fiber lasers have become an important alternative that can match and even enhance the performance of currently used lasers while reducing the complexity, costs and instability.

Optical fibers, which are the main components of fiber lasers, were first developed just as a substitute for conventional cables since they offer much less attenuation in carrying signals over long ranges. The ability of optical fibers to confine light and transform it around bends and loops has always fascinated researchers and after realizing that it offers great beam qualities, which is a vital parameter for many laser applications, researchers started to find innovative ways to utilize the optical fibers to laser systems [12]. Despite the advantages of optical fibers, they did not attract very much attention until the availability of high brightness laser pump diodes in 1980 [13] and the development of efficient rare-earth doped fibers [14, 15]. After the application of optical fibers in laser systems, unprecedented improvement has been observed and numerous types of fiber lasers have been developed based on different purposes such as maximum peak power, pulse energy and repetition rate despite the relatively short history of optical fibers [1, 16–23].

With the continued developments, the pulsed operation has spawned new fields of scientific investigation and expands its application potential, so today lasers with pulsed operation still remain the subject of active research [24–26]. The utilization of fiber lasers for an energetic ultrashort pulse generation was a difficult task for the researchers because of the limitations engaging in conflict with a geometry of the fiber such as the nonlinear effects and damage of fiber caused by the confinement of the beam into small volumes [27]. After overcoming the limitations by using smart techniques and designs like chirped pulse amplification and highly doped gain fiber, pulse energies and peak powers close to solid-state lasers can be achieved and ultrashort pulse fiber lasers became more than just a research topic in the laboratory and have seen continuous development and expansion of

their application potential [21, 25]. After continuous development of ultrafast lasers and becoming a well-developed tool, the prejudiced thoughts about ultrashort fiber lasers as being complex and unreliable has been changed and they are being considered as a tool for industrial solutions. Today, ultrafast fiber laser market provides much promising technology and application trends, and falling prices for applications as diverse as medicine, telecom, precision metrology and material processing as new applications of fiber lasers are being continuously developed.

1.2 Overview of Laser Material Interaction

Applications of ultrafast laser material processing have become extremely numerous [28–35], enabled by rapid developments that have taken place in the field of ultrafast lasers, particularly, in Yb-doped fiber [20,21,23] and solid state lasers [6] in the past decade. Despite these improvements, ultrafast material processing is still complex, costly and quite slow in terms of material removal [36] rendering ultrafast lasers uncompetitive compared to mechanical techniques for many applications [34].

Optical energy is absorbed because of the interaction between the laser beam irradiation and the bound electrons of the material. If the electron is bound the the lattice structure of the material, then this energy will be transferred to the structure which causes the vibration of the structure by a sufficient flux of photons. This effect can be detected as a heating of the material. With a greater amount of photons, those vibrations reach a sufficient level for breaking the bonds of the material structure which starts with melting and followed by evaporization. Then the vapour is ionized and forms a plasma and the finally the solid starts to ionize introducing the Coloumb forces to remove the material. The last condition requires immense power level for exploiting. Therefore, in addition to optical energy, equally important attribute is the type of energy delivery, such as continuous or pulsed deliveries and pulsed lasers can be charaterized by increadibly high pulse energies compared to the continuous wave lasers. As a result of

this, pulse duration together with the power density (W/cm^2) directly affects the chemical and mechanical interactions occurring inside the material upon given an incident beam. These interactions are mainly photochemical, thermal, plasma induced, photoablation and multiphoton absorption.

The dynamics of energy deposition on to the target by sub-ps pulsed laser interactions can be categorized in two ways. First one, the pulse can deposit its energy over a target on timescale that a shorter than electron-lattice relaxation time around sub-ps level. The incident pulse transfers its energy to the bound electrons while keeping the ions practically cold because of an insufficient time for energy transferring from electron to lattice. When the incident pulse is turned off then the transfer of the thermal energy from electrons to lattice starts which is a strongly nonequilibrium process. The second case is that using an extremely short pulse durations with very high pulse energies for exploiting the nonlinear and multiphoton absorption processes. Due to the strong nonequilibrium states for both cases, the generation of molten material and heat affected zone is reduced. Therefore, laser systems with the pulse duration of femtosecond are commonly preferred in application areas like precise micromachining or ophthalmology due to preventing collateral damaging. These systems are typically operating with a low power and at low repetition rate which causes a very low rate of ablation. This situation is tolerable when it is applied to the small volumes, but not to the larger material removal process.

There are several key parameters for increasing the ablation efficiency. First one is the selecting the correct wavelength range wih a maximum absorption value which ensure a high energy transfer into the interaction volume with a maximum efficiency for exploiting the ablation. The second one is the short pulse duration to maximize the pulse energy and reducing the heat conduction around the interaction volume. The third one is the repetition rate. Increasing the repetition rate significantly increase the ablation efficiency and reduces the heating of surrounding regions.

The common used technique for material removal with laser irradiation is the

plasma mediated ablation which is achieved by ultra-short laser pulses with extremely high peak intensity. This process leads to nonlinear absoprtion in the material, which then leads to ionization of the atoms and the molecules at the focal spot and results in plasma formation. Exceeding the power density threshold yields very well defined removal of material with no evidence of thermal and mechanical damage. If laser illumination at the focus continues, within few picoseconds very large free electron density is obtained, which has the essential role in plasma ionization. Reaching the power density threshold for optical breakdown is important because, even inside a weakly absorbing medium, the induced plasma makes it possible to remove the material and the process becomes wavelength independent.

The use of ultrafast lasers allows precise ablation without any thermal damaging within the light-matter interaction region for wide-ranging application areas. However the potential of the ultrafast lasers is limited by the low speeds of material removal and an extremely high peak intensity is required for exploiting the ablation process which increases the complexity and the cost of the laser design. A new regime of laser-material interaction which is called as "ablation-cooled laser material removal" has been proposed by our group [1] with the potential to overcome these limitations. During the ablation, heat energy within the ablated volume is carried away from the system. This effect forms the basis of ablation cooling. In this regime, the repetition rate has to be high enough to prevent the targeted spot size to cool down substantially by heat convection while the next pulse arrives. This new regime of laser-material interactions has several interrelated advantages: (i) the required individual pulse energy for exploiting ablation cooling is reduced at the high repetition rate because most of the residual heat deposited by each pulse will not have yet time to diffuse out of the volume to be ablated by the time the next pulse arrives (ii) lower ablation threshold comes with major side benefits such as preventing plasma shielding, cavitation bubble formation and self focusing. The development of new compact laser systems designed for exploiting the ablation cooling effect and the advances made in material processing with ultrashort laser pulses (in many cases even under atmospheric conditions) are essentials to stimulate the use of the ultrafast laser technology not

only inside the research laboratory but also outside research and development.

In terms of the developed and deployed laser technology, ultrafast laser ablation experiments have traditionally dominated by solid state lasers, particularly Ti:sapphire lasers, which typically produce tens of μJ to mJ levels of pulse energies at kHz or lower repetition rates [37–40]. Meanwhile, the applications of fiber lasers are emerging with major inherent practical advantages, such as compact size, lower cost, superior robustness against environmental fluctuations as well as adaptability to highly integrated design which distinguished them from their solid state counterparts. However, the performance of fiber lasers is still lagged behind the solid state lasers in terms of attainable pulse energies, which is an important parameter for an efficient material ablation. Also, the high repetition rates have a crucial role for fully exploiting the ablation cooling effect and achieving an efficient ablation process [41]. The increase in the pulse energy of fiber lasers has been fascinated many researchers all around the world due to inherent advantages of fiber medium and they have exerted much effort to push the limits of this active medium based on silica fiber. The attainable repetition rates, on the other hand, are still limited by the average power of the system due to the thermal loadings. Recently, a new operating mode of fiber lasers has been demonstrated, i.e., the burst mode operation [2, 42, 43]. In ultrafast burst-mode operation, which was invented by R. Marjoribanks, et al. [44], bursts of pulses are generated, each burst consisting of a number of temporally closely spaced (order of 10 ns) pulses. This new operating mode allows the system to operate at high repetition rates over a relatively short time keeping the pulse energy high close to the level of solid state counterparts and the average power low. Through the use of ultrafast pulses delivered in burst mode, a completely new interaction regime opens up that holds great potential for use of the laser as a precise scalpel for material removal applications, and the possibility to overcome the limitation of achieving an efficient ablation rate with the help of the high repetition rate and pulse energies [45,46]. This mode of operation has already been shown to increase the ablation rate for metals [18,41] and hard tissue, *e.g.* tooth samples [1,45], as compared to the application of pulses at a lower repetition rate.

Since the laser technology required to demonstrate ablation cooling does not

exist, we have developed special fiber lasers [2, 42, 47, 48] for exploring the advantages of this new laser-material interaction regime. Ablation cooling becomes significant above a certain repetition rate, which depends on the thermal diffusivity of the target material. It requires trains of relatively high energetic pulses at such high repetition rates corresponding to prohibitively high average powers. Besides, the benefits of simply scaling up the repetition rate are severely limited by the finite speed of beam positioning devices, such as galvonometric scanners. As a consequence of these requirements, we have implemented the burst-mode operation technique which substantial benefits of material processing with burst-mode operation already has been reported [41, 44, 45]. However, the advantages of the ablation cooling effect by implementing the burst mode operation have recently been recognized by our group with a detailed investigation of different target materials. [1].

This thesis contains a sequence of the development of fiber laser systems that will open the way for exploiting the ablation cooling effect. Therefore, two step procedure is followed in the developing the burst-mode fiber laser systems. First, the design and construction of the mode-locked oscillator generating a train of pulses with a high repetition rate and second, the construction of the burst-mode amplifier system. Although the physics of the ablation cooling effect is valid for every target material, materials have wavelength dependent absorption and scattering, which are quantitative measures of how deep a laser beam may penetrate into the material and deviate from its straight trajectory. Therefore, for efficient material and tissue processing, two different wavelength regimes are covered emitting 1 μm and 2 μm respectively.

1.3 Overview of Fiber Lasers

With the rise in popularity and capability of fiber laser systems, this direction represents an important modern trend in laser technology. Therefore, this section outlines the history of and reasons for the use of fiber lasers, which are a special type of solid state lasers but distinguished from all the other laser system

generations by being much more practical in many applications.

Ultrafast lasers have a supporting role for many photonic systems like applications in industrial and medical facilities as well as for scientific research. As one type of ultrafast lasers, ultrafast fiber lasers have been playing a crucial role in the development of ultrafast applications due to their compactness, inexpensive components, ease of operation and reliability compared to their bulk solid state counterparts. The scientific interest in fiber lasers stems from the rich nonlinear dynamics. Industrial interest largely comes from their practical advantages. However, fiber lasers have their own disadvantages, preventing the use of fiber lasers in general ultrafast applications when they are compared to their solid state counterparts such as attainable pulse energies available directly from the fiber cavity, limited pulse durations and difficulties in scaling up the fundamental repetition rates.

Although, ultrafast fiber lasers have great potential to be routinely used for a variety of applications, compared to their solid state counterparts, fiber lasers have been a newly emerged technology and their performance has historically lagged behind that of solid state lasers. For improving the performance of fiber lasers, amplifier systems have been required which in some cases just increase the complexity and cost. As an example, one of the drawbacks of fiber laser is that there is a limited choice of gain media with much narrow gain bandwidths than solid state lasers. This situation fundamentally limits the attainable pulse duration from a fiber oscillator without innovative ideas. As a result, solid state lasers still dominate the application fields. Initially, ultrafast fiber lasers have gained an interest due to their adaptability to highly integrated designs. The potential advantages of ultrafast fiber lasers have motivated researchers to overcome the problems. Since then, considerable research activities have been carried out to improve the performance of fiber lasers with respect to their limitations in pulse duration, pulse energy, and fundamental repetition rate .

For reliable self-starting pulse operations, fiber oscillators require saturable absorbers. Such fiber oscillators based on polarization maintaining fibers are highly desirable especially for commercial applications for achieving self-startign and

stable pulse operations. Those fiber oscillators have a capacity to generate pulse durations around 100 fs [49]. Despite the robustness of saturable absorbers, each fiber laser gain medium can require different absorber design which may increase the complexity of the setup. Therefore, fiber oscillators without semiconductor saturable absorbers have been investigated. Stable and the self-starting pulse operation can be initiated by using many different techniques like inserting an electro-optic modulator [50]. Based on whether or not the mode-locking is induced by an electro-optic modulator, the ultrafast fiber oscillators can be categorized into actively mode-locked and passively mode-locked lasers, operating without any modulators but incorporate components that act on the amplitude of the oscillating pulses. The rich interplay of dispersion, nonlinearity, gain and loss in short pulse fiber gives rise to many different pulse shaping mechanisms such as soliton-like, dispersion management, nonlinearity management, self-similar and soliton-similariton pulse propagation. These effects have been a target for study at fundamental level, route to energy scaling as well as generation of shortest pulse duration. The theoretical and experimental discover of self similar and dissipative soliton evolutions added an additional degree of freedom to the formerly well known soliton evolution whereby an achievable pulse energy of a soliton in a fiber laser which is 10-100 times lower than in a solid state laser. The demonstration of ultrashort fiber lasers to reach the performance of Ti:sapphire laser needed two decades of time for fully understanding of short-pulse generation and high pulse energy. A dissipative-soliton laser was the first fiber laser that reached the power level of Ti:sapphire laser [51] which generated the pulse duration of sub 100-fs pulses with the pulse energy of 20 nJ in 2009. This laser consisted of mostly Yb-doped fiber and a spectral filter dominated the steady state pulse shaping.

In fiber lasers, light is propagating in the core region for long distances and experienced accumulation of excessive nonlinear phase shift due to small confinement area when they are compared to other solid state lasers. Hence, the nonlinear effects become inevidable and the main concerns are causing limitations for achieving an attainable high pulse energy in fiber laser design. This limitation can be overcome by the chirped pulse amplification (CPA) technique

and applying large mode area fibers. In the simplest form, CPA technique consists of pulse stretcher and compressor part with doped fiber as a gain medium in between. This technique can be used for achieving the largest possible pulse energy. Subpicosecond pulses with pulse energies of around μJ can be obtained by using this technique with conventional rare-earth doped fiber amplifiers with a core diameter of 5-10 μ [2, 52]. Such pulse energy levels can be used for many applications, especially in ophthalmology [53].

Precise micromachining applications with femtosecond pulses with the superior hole quality compared to microdrilling with longer pulse durations require pulse energy of mJ ranges [41, 44, 54]. Fiber lasers with femtosecond pulse duration and millijoule pulse energies can be obtained with the usage of large mode area fibers. Nonlinear effects depend on the peak intensity inside of the fiber and threshold of nonlinear efects is reduced by decreasing the optical intensity by increasing the interaction area with the fiber medium. Therefore large mode area fibers become suitable canditates for high average power and pulse energy setups. The easiest way for increasing the mode area of optical fibers is expanding the core diameter and the method is effective for core diameters in the range of 20-50 μm [17, 55, 56]. Due to the multimode nature of large mode fibers, single mode operation can be excited by appropriate mode matching at the input [57] or eliminating the higher order modes by bending [58] or channelling out higher order modes with satellite cores [59]. After the realization of large mode area fiber's advantages, achievable pulse energies from femtosecond fiber laser systems have been continuously increased and the highest obtained pulse energy from a single fiber amplifier was reported as 2.2 mJ [60].

The most common application areas of these fiber laser systems are material and tissue processing. However, ablation speed still remains as a main obstacle despite the unique possibilities of fiber laser systems. High repetition rate pulses can be a powerful approach for abolishing this obstacle [45] which is still challenging for fiber laser technology. Therefore, there is a considerable desire for achieving pulse generation at very high repetition rates beyond the range of active and passive mode-lockings [61, 62]. Many different approaches have been

reported to achieve higher repetition rate pulses including a very short laser cavities with large mode frequency separation [63] or producing multiple pulses in each round trip [64].

Although some challenges lie ahead like nonlinearity in spite of generating a lot of rich physics and novel concepts which becomes a main obstacle to develop many new fiber laser ideas, fiber lasers challenges currently held views on their bulk solid state counterparts because of their compactness, their inexpensive production and their high reliability arising from a compact setup. Consequently, the aim of this Ph.D. thesis is to develop compact, simple to operate and cost-efficient all-fiber integrated ultrafast lasers, so for obtaining a high technical performance from a fiber laser systems without loss of any practical advantages.

In Chapter 2, the theory of fiber lasers is discussed in general way starting from the laser gain and followed by introducing the pulsed operation, including mode-locking theory which is a pulse generation mechanism in the fiber laser cavity. After a brief explanation of laser amplification process of signals in a fiber configuration and introducing different gain media corresponding to different wavelength regimes, pulse propagation in optical fibers is explained briefly including the Nonlinear Schrödinger equation (NLSE) which is essential for investigating the pulse dynamics inside the laser cavity.

The third chapter of this thesis is dedicated to fiber oscillators generating high repetition rate pulses with pulse durations around picoseconds as seed sources for amplification and achieving high pulse energies. We reported the experimental results in scaling up repetition rates of two different fiber oscillators. The first laser was built at 1 μm wavelength range with Yb gain medium. For the design of Yb-doped fiber oscillator, we preferred to build all normal dispersion mode-locked Yb doped fiber oscillator with a fundamental repetition rate of 100 MHz. In this regime, the usual balance between nonlinearity and dispersion was replaced by nonlinearity and dispersion acting together and balancing against the spectral and temporal filtering by both the filter and the saturable absorber. In this oscillator design, the fundamental repetition rate was limited by two challenges: (i) in practice, the cavity length was limited by the physical size of the optical

components which were used in the laser cavity, (ii) when we looked at the most fundamental way, there was a threshold power for stimulating passive mode-locking mechanism. Therefore, various approaches have been investigated to achieve stable high repetition rate pulses beyond the limits of the optical cavity. Depending on this purpose, a second oscillator design was built based on a novel mode-locking principle. Dissipative four wave mixing (DFWM) was the main mechanism governing the formation of a remarkably stable train of pulses at different dispersion regimes [65]. We achieved stable mode-locked operation at a repetition rate of 100 GHz which was determined by the free spectral range of the Fabry-Perot filter inside the optical cavity. In this design, we preferred Erbium as a gain medium and net cavity dispersion (β_{net}) was varied from normal to anomalous dispersion regimes.

The 4th chapter contains experimental studies on the amplification of burst signals, which were generated with the Yb-doped fiber oscillator described in chapter 3. From a material processing point of view, pulse energies above 10 μJ is highly desirable to obtain efficient processing, while keeping the pulse duration 15-20 ps to reap the benefits of ultrafast ablation. Therefore, the laser setup was designed based on creating sub-20 ps pulses directly to avoid the use of external compression. Additionally, a detailed characterization of the burst repetition rate and associated ASE generation that can be achieved under continuous pumping were reported. ASE generation was monitored directly in a special time-gating measurement setup. We found that pulsed pumping was not required at burst repetition rates above 200 kHz to maintain an ASE ratio of less than 2 %.

The fifth chapter of this thesis is devoted to develop a fiber laser amplifier system operating around 2 μm for transparent material and tissue processing applications. Our know-how on Yb-fiber laser amplifier systems operating at 1 μm which was explained in chapter 4 transferred to the fiber laser systems operating around 2 μm. Therefore two-step procedure was implemented. First one was the design and construction of the high brightness pump sources at 2 μm wavelength regime by a spectral beam combining of high power Tm-doped fiber lasers based on WDM cascade design. Signal beam combining of Tm-doped fiber lasers can increase the laser output power while simultaneously maintaining

the single mode beam quality. The constituent lasers were operating at the wavelengths of 1920, 1949, 1996 and 2030 nm and in-house-made WDMs were used for combination of these different wavelengths with cascaded laser concept with 69% overall coupling efficiency. At the end, we obtained all-fiber truly single mode power combining with high power Tm-doped fiber lasers. Continuous wave output power of 38 W was demonstrated using four-channel fiber oscillators with the spectral beam combining method. After building pump sources, the construction of Ho-doped fiber amplifier was implemented as a second step. We proposed temperature management in Ho-doped fiber amplifiers by employing dual-wavelength pumping. Our concept provides a solution based on all-fiber laser design and a configuration using different pump absorption coefficients along the cavity can improve the laser efficiency and reduce temperature gradients in the fiber to some extent. As a first implementation, we obtained an average power of 9 W from Ho-doped fiber amplifier resulted in an efficiency of 68% with the dual wavelength pumping concept. Our results can however be applied to cases with higher output power for continuous and pulsed operation.

The final chapter provides the concluding remarks.

Chapter 2

Principles of Laser Operation

There are numerous types of lasers developed over the past 50 years for various investigations and needs. Despite their various types, the basic working principle is the same for all laser systems. The general overview of lasers and their historical developments have been already discussed in the previous chapter. Therefore, in this chapter, the basic principles involved in the generation of laser will be discussed basically.

2.1 Laser Amplifiers

First of all, it is better to introduce simplified introduction to principles of lasers in order to show the feasibility of mode-locked operation. The basic laser structure contains three main parts: (i) gain medium, (ii) a pump mechanism, (iii) a mechanism for providing an optical feedback. The gain medium is a material which can be solid, liquid or gas, and it has a property to amplify the light wave which is passing through it with the help of stimulated emission. However, this process requires an energy which can be supplied by a pumping mechanism and the pumping energy can be obtained from an electrical current, a light at different

wavelengths or more exotic sources such as chemical or nuclear reactions. An optical cavity is used as a feedback mechanism. Basically, an optical cavity consists of a pair of optically parallel and highly/partially reflecting/transmitting mirrors. The gain medium is placed between those mirrors and light starts to propagate back and forth in the cavity, passing through the gain medium and being amplified in each time. The amplified light is emitted through the transmitted mirror at each reflection.

The working principle of laser relies on the stimulated emission. Let us imagine a gain medium contains only two energy levels such as the ground state and the upper state. Generally, all electrons stay in the ground state and they are excited to the upper state by applying an energy into the system, then just after a few nanoseconds after their excitation, they return back to the ground state by emitting photons. The stimulated emission is the process whereby the interaction of a photon which has a specific frequency, phase and polarization state with an excited electron and causing it to return back to the ground state. The freed energy which is equal to the energy difference between the states involved in this process, transfers to the electromagnetic field and creates a new photon which is an identical with the first one.

Generated light from an optical cavity can be amplified by Rare Earth doped optical fiber with the active ions which are doped in the core region of the fiber. Optical fiber amplifiers are like optical cavities without a feedback. Amplification process is a linear process which increases an amplitude of an input signal by a fixed factor and this factor is called as an optical gain. Within the amplifier gain bandwidth, optical gain is constant for all frequencies in an ideal amplifier. However, in a real world, gain of the amplifier depends on the frequencies and amplification process occurs until saturation occurs.

Usually lanthanides have been used as active dopands in optical fibers such as Erbium, Ytterbium, Neodymium or Thulium. These dopands consists of 14 similar elements with atomic numbers in the range of 58 to 71 and those atoms become triply ionized when they are doped into the silica or other glasses [27]. The optical properties of those active ions are determined by their partially filled

inner 4f shells and electrical dipole transition between the different energy levels of the 4f electrons are forbidden due to the even parity of these transitions. When those atoms are doped into the host material, then their spherical symmetry is disturbed and electric dipole transitions become possible. This process provides a lasing in the desired wavelength range with respect to the type of doping elements. Table 2.1 depicts the rare earth dopands with a host material and their emission wavelength range.

Rare Earth Doped Elements		
Elements	Emmission wavelength (nm)	Host materials
Neodymium (Nd)	1.03 - 1.1 μm 0.9 - 0.95 μm 1.32 - 1.35 μm	Silicate and phosphate glasses
Ytterbium (Yb)	1.0 - 1.1 μm	Silicate glass
Erbium (Er)	1.5 - 1.6 μm 2.7 μm 0.55 μm	Silicate and phosphate glasses, fluoride glasses
Thulium (Tm)	1.7 - 2.1 μm 1.45-1.53 μm 0.48 μm 0.8 μm	Silicate and phosphate glasses, fluoride glasses
Praseodymium (Pr)	1.3 μm 0.64 μm 0.52 μm 0.49 μm	Silicate and fluoride glasses
Holmium (Ho)	2.1 μm 2.9 μm	Silicate and fluorozirconate glasses

Table 2.1: Common laser-Rare Earth ions with host glasses and important emission wavelengths [4].

2.1.1 Gain Dynamics

Despite possessing different emission, absorption wavelength and application areas, all these Rare Earth doped fibers have similar gain dynamics. Depending on the energy levels of dopands, lasing scheme can be categorized as three level and four level scheme. In both cases, working principle is almost same which dopants absorb pump photons to excite their electrons to an excitation state. Then relaxed slowly back into a lower energy state without radiation. The stored energy is used for signal amplification. The main difference between three-level and four level system comes from ending point of the transitions. In the three-level system, the laser transition ends at the ground state. On the other hand, in the four-level

scheme, lower lasing level is well above the ground state (see Fig. 2.1).

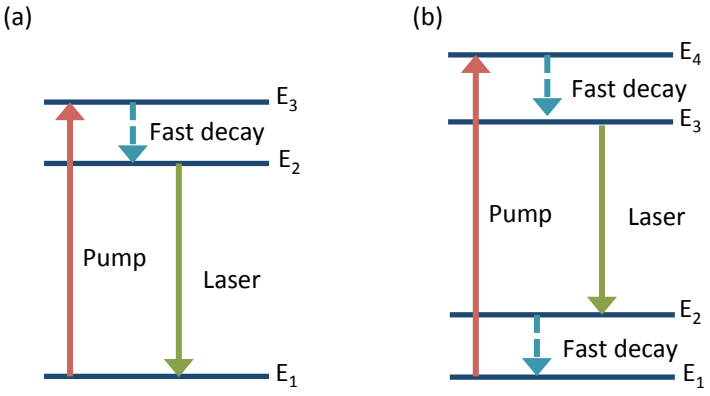

Figure 2.1: Illustration of (a) three-level and (b) four level lasing schemes.

Despite this different energy transition between levels, in order to obtain desired gain and amplification from both laser systems, getting a higher population inversion is the common point which means creating higher ion density in the upper energy level depending on the pump power. Therefore, three-level and four-level systems are solved based on the same method. Modelling of these amplifiers are possible with rate equations where the population levels of excited and ground states as well as the pump and signal powers are calculated [66].

For the three-level lasing scheme, N_1, N_2, N_3 are defined as a population for ground, first and second energy levels respectively. Then changes in those populations with respect to time because of the presence of absorption, spontaneous and stimulated emission are calculated by rate equations in the steady state [67].

$$\frac{\mathrm{d}N_1}{\mathrm{d}t} = W_{signal}(N_2 - N_1) + W_{pump}(N_3 - N_1) + \frac{N_2}{\tau_{21}} \tag{2.1}$$

$$\frac{\mathrm{d}N_2}{\mathrm{d}t} = W_{signal}(N_1 - N_2) + \frac{N_3}{\tau_{32}} - \frac{N_2}{\tau_{21}} \tag{2.2}$$

$$\frac{\mathrm{d}N_3}{\mathrm{d}t} = W_{pump}(N_1 - N_3) - \frac{N_3}{\tau_{32}} \tag{2.3}$$

where τ_{21} is the upper state life time for the transition from second energy level to the first energy level which is called as a spontaneous emission and τ_{32} represents the upper state life time for the transition from third energy level to the second one called as a fast decay as can be seen in the Fig. 2.1. W_{signal} and W_{pump} stand for the signal absorption/emission probability and the pump absorption probability and they can be calculated as:

$$W_{signal} = \frac{P_{signal}}{S_{core} h\nu_{signal}} \sigma_{signal} \tag{2.4}$$

$$W_{pump} = \frac{P_{pump}}{S_{core} h\nu_{pump}} \sigma_{pump} \tag{2.5}$$

where P_{pump} and P_{signal} are representing the power of signal and pump. S_{core} is the core area of the active fiber where active ions are doped. σ_{signal} and σ_{pump} define the emission/absorption cross sections for signal and pump respectively and those cross sections give a probability of a single atom interaction for emission/absorption at a specific frequency. Therefore Eq. 2.4 and Eq. 2.5 are dimensionless quantity but they define the probability for a photon flux interaction with a single atom. Also note that W_i is the same for stimulated emission or absorption.

Creating population inversion between two lasing energy level (see Fig. 2.1) is the main point in order to obtain gain as mentioned from the beginning of this section. This situation requires more population in the second energy level and degree of population inversion is given in the following equation;

$$n = \frac{N_2}{N_2 - N_1} \tag{2.6}$$

Gain coefficient of a laser medium depends on the population difference n which depends on the transition rate W_i and transition rate depends on the flux density that is to be amplified. The gain coefficient represents the net gain in

the photon flux density per it lenght of the medium. Based on Eq. 2.6, then the optical gain can be calculated as;

$$g = \sigma(N_2 - N_1) \tag{2.7}$$

The population difference between two energy levels which lasing process occurs decreases in the presence of stimulated emission. This phenomenon is called as a gain saturation. Therefore population difference with the dependence of gain saturation becomes;

$$n = \frac{N_0}{1 + \phi/\phi_s(\nu)} \tag{2.8}$$

where N_0 defines the population difference with the absence of amplifier radiation and $\phi_s = \tau_s\sigma(\nu)$. Then we can write the optical gain with the dependence of gain saturation as;

$$g = \frac{g_0}{1 + P/P_s} \tag{2.9}$$

where g_0 is the small signal gain. P and P_s represent the signal power and saturated signal power respectively. It is more obvious in the Eq. 2.9 that the gain coefficient shows a decreasing behaviour as the signal power increases. This behaviour is known as a gain saturation because of depopulation of excited state.

In the fiber amplifier design, active ions doped in the core of the fiber can be pumped by coupling the pump light into the core of the fiber. This method provides the good overlap between the pump and the active ions in the core area since the light is guided in this core. Despite this advantage of this pumping scheme, coupling the pump into the fiber core requires a single mode beam quality. Therefore, the double-clad pumping technique generally is preferred for diode pumped high power fiber lasers and amplifiers. In this technique, the pump is propagating in the second cladding layer which surrounds the cladding of the

fiber core as a second waveguide structure for a pump. This section of the fiber has a relatively larger diameter, which supports many fiber modes, so high power laser diodes with relatively low beam quality can be used and coupled into this waveguide structure easily. In spite of technical and practical advantage of the cladding pumping technique, the pump absorption is reduced because of the smaller overlap area between the pump and active ions in the fiber core because only meridional rays are absorbed by the active ions and obviously the screw rays cannot be absorbed. This reduction ratio depends on the ratio between the area of the fiber core and the outer cladding.

In the following subsection the properties of Erbium, Thulium and Ytterbium doped gain fibers are described, because the experiments in this thesis were based on these fibers.

2.1.2 Erbium gain fibers

As mentioned in the previous section, Erbium is a chemical element which belongs to the rare earth elements and is used for constructing a fiber laser and amplifier system in the eye safe region where optical absorption by water in the eye prevents power from reaching the retina ($> 1400nm$). Generally silicate and phosphate glasses are used as a host material for Erbium for both bulk lasers and fiber lasers and amplifiers. Erbium gain provides a broad bandwidth and high gain which makes it a great candidate for generating and amplifying femtosecond pulses. The optical properties of Er ions are determined by the energy levels for 4f electrons which have a crucial role for relevant applications. The following figure (Fig. 2.2) shows the energy levels of erbium ion and their sublevels which are caused from Stark splitting for Er ions in silica glass.

Due to the low non-radiative decay rate at the level of $I_{13/2}$, the radiative decay at that level becomes dominant and also this level has an extremely long lifetime about 10 ms which provides a high population inversion between $I_{13/2}$ as an excited level and $I_{15/2}$ as a ground level. Consequently, Erbium doped fibers become the best candidate for the optical gain [68].

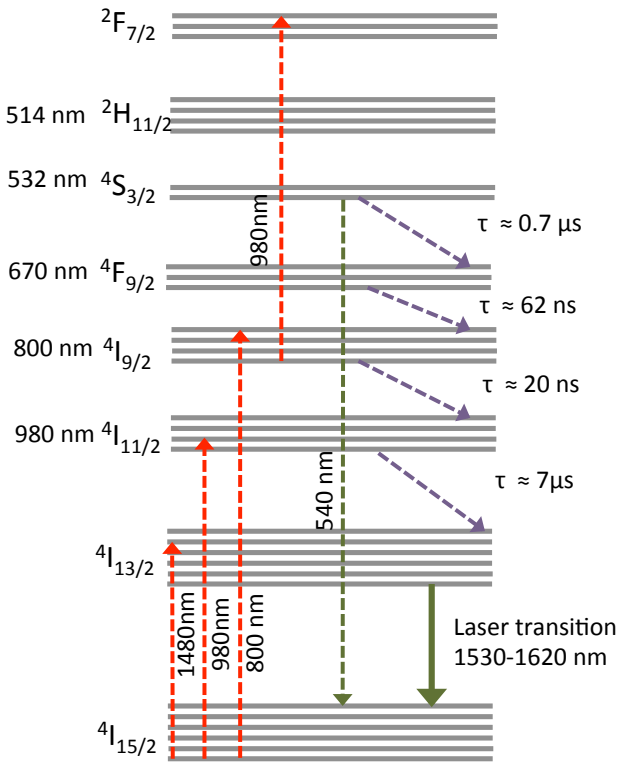

Figure 2.2: Illustration of energy levels of the triply ionized erbium ion with some pump, excited state and non-radiative transitions. The main laser transition is indicated by a solid green arrow.

2.1.3 Ytterbium gain fibers

Erbium as a gain medium has attracted a great interest since the beginning of the fiber lasers invention, yet after increasing necessity for high peak power in some application areas like telecommunication, erbium doped amplifiers have experienced some practical issues in obtaining maximum efficiency [69]. On the other hand, Ytterbium doped fiber amplifiers provide amplification over a very broad wavelength range more than 40 nm with a relatively higher efficiency than Erbium doped fiber amplifiers up to 80 % [66]. This property makes Yb doped fiber amplifiers appropriate candidates for high power applications. Their excellent power conversion up to 80% and high doping levels provide a high gain even in a very short length of gain medium.

The energy levels of Yb ion can be seen in Fig. 2.3 consisting of only two

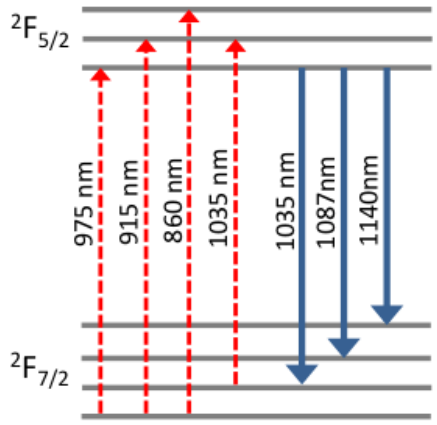

Figure 2.3: Energy levels of Ytterbium ion with a ground state and an excited state including the Stark levels of these manifolds are indicated. The main laser transition and pump transitions are shown as blue solid lines and red dashed lines respectively.

distinct energy levels as a ground state and an excited state with their Stark splitting. Also wavelengths of excited state absorptions and signal emissions are indicated. The lifetime of the excited state is approximately 0.8 ms - 1.5 ms which depend on the silica fibers [66]. Yb doped gain medium behaves like quasi-three level system which is the intermediate situation between three level and four level systems, particularly at shorter wavelengths. Additionally, Yb-doped gain fiber has a small quantum defect which allows for a very high power efficiencies of lasers and it also reduces the thermal effects in high power applications.

2.1.4 Thulium gain fibers

Among Erbium and Ytterbium ions, utilization of Thulium ions is newly emerged, yet it is a rapidly expanding field and has become a top choice for eye safe high power applications at the wavelength range of $2\mu m$. Beside the advantage of the eye safe region, Thulium ions have the widest potential lasing bandwidth ranging from 1720 nm to 2180 nm which makes them a great candidate for applications including ultrashort pulse lasers and spectral beam combining. In addition, Thulium doped lasers with a wavelength around $2\mu m$ are suited for nonlinear

frequency conversion into the mid-IR which is an important range for various application areas such as spectroscopy, bio-imaging, medical and defense. Despite the technical difficulties which arise from a newly emerged technological frontier, Tm-doped lasers come to the front as the best choice for reaching high powers and pulse energies in the eye safe regime with a low quantum defect and subsequently a low thermal load because of efficient cross relaxation process (see Fig. 2.4) [70].

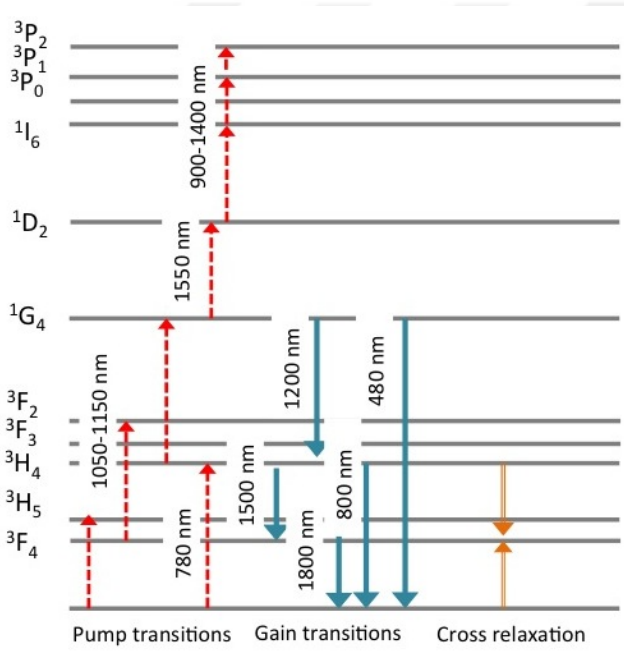

Figure 2.4: Illustrating the energy level diagram for Thulium ion with pump and signal transitions including cross relaxation process.

The four energy levels of Tm ion ($^3H_6$, $^3F_4$, $^3H_5$, $^3H_4$) are the most important levels for the operation of eye safe Thulium lasers as can be seen in Fig. 2.4. The individual energy level structures are broadened into many sublevels when Tm ions are doped in glasses due to the local electric field caused by neighboring atoms which is experienced by a particular ion in the glass background material [71]. This local electric field depends on intensity and is varied by random inhomogeneties and variations in the glass. Therefore, different ions have slightly different energy levels and transition wavelengths because of the Stark effect [72] and this phenomenon is known as an inhomogenous broadening and dominates the mechanism for creating a large bandwidth of the Thulium ion [71]. The Stark

splitting is not indicated in the Fig. 2.4.

The laser transition starts from the sublevels of $^3H_6$ as a ground state to the $^3F_4$ and provides broad emission bandwidth varying between $1.6\mu m$ to $2.2\mu m$. As seen in the Fig. 2.4, the energy levels of Tm ion provides numerous potential pump bands from the ground state to the other energy levels. Additionally, the high phonon energy of silica helps to make the multiphonon emission from these excited levels to the $^3F_4$ very quickly. Beside all these emission transitions in Tm ion, the case of pumping at 790 nm can lead to the advantageous cross relaxation process, which enhances the quantum efficiency of Tm doped lasers.

The cross relaxation process requires interaction between two identical ions to exchange their energy between an excited state electron with a ground state electron, so that both end up in some intermediate level (see Fig. 2.4). The energy transfer from an excited level electron to a ground state electron is known as Förster energy transfer which is a non-radiative process. A dipole-dipole interaction of two identical ions is caused the energy transfer, so that this transfer strongly depends on the distance between two ions and the dopand concentration becomes a crucial parameter for the quantum efficiency [73].

2.2 Pulse Propagation in Optical Fibers

When one is dealing with the linear wave equation, the response of the material is assumed as a linear function of light intensity and the dependence of the index of refraction on wavelength like dispersion is simply ignored. However, while dealing with the pulses propagating inside a fiber, the response of the material should be considered. Ultrashort pulses have large spectral bandwidths and high peak powers, which affect the material properties of the propagating medium. Pulse propagation in optical fibers can be accurately modeled by one or more coupled partial differential equations which, for historical reasons, are called the nonlinear Schrödinger equations (NLSE). By solving the NLSE, the pulse evolution in various fiber system can be predicted. The derivation of the NLSE equation from the

well-known Maxwell's equation is well covered in numbers of textbooks such as Ref [27, 74]. The final equation obtained through a somewhat lengthy derivation is;

$$\frac{\partial A}{\partial z} + \frac{\alpha}{2}A + i\frac{\beta_2}{2}\frac{\partial^2 A}{\partial t^2} - \frac{\beta_3}{6}\frac{\partial^3 A}{\partial t^3} = i\gamma[|A|^2 A + \frac{i}{\omega_0}\frac{\partial |A|^2 A}{\partial t} - T_R A\frac{\partial |A|^2}{\partial t}] \quad (2.10)$$

The Eq. 2.10 gives a description about the evolution of the slowly varying envelope function $A = A(t, z)$ in a third order nonlinear medium like a optical fiber ($\chi_2 = 0$ and $\chi_3 \neq 0$). t and z represent the local time and the propogation distance respectively. In left hand side of the Eq. 2.10, α is the gain/loss coefficient. β_2 and β_3 stand for coefficients of the Taylor expanded propagation constant $\beta(\omega)$ around the carrier frequency (ω_0) which can be seen in the following equation;

$$\beta(\omega) = \beta_0 + \beta_1(\omega - \omega_0) + \frac{1}{2}\beta_2(\omega - \omega_0)^2 + \frac{1}{6}\beta_3(\omega - \omega_0)^3 + ... \quad (2.11)$$

In the Eq. 2.11, β_2 and β_3 are referred as the group velocity dispersion (GVD) and third order dispersion (TOD) coefficients respectively. Higher order terms can be neglected in the Eq. 2.10 because their effects on the pulse propagation are negligible in most cases especially for fibers. γ is the nonlinear coefficient, which can be defined as $\gamma = \omega_0 n_2/(cA_{eff})$ where n_2 represents the nonlinear index coefficient and A_{eff} is the effective mode area. In the right hand side of the Eq. 2.10, the second and the third terms are referred higher order nonlinear terms which are related to the self steeping and the raman self frequency shift respectively. For a relatively longer pulse duration 100 fs with a low peak power, which is valid for most of fiber lasers, we can ignore TOD and higher order nonlinear terms. Also gain/loss term may become negligible while the pulse is propagating inside the optical fiber. After eliminating these terms, then we can obtain the famous NLSE;

$$\frac{\partial A}{\partial z} + i\beta_2\frac{\partial^2 A}{\partial t^2} = i\gamma|A|^2 A \quad (2.12)$$

The NLSE (Eq. 2.12) contains only two phase modulation terms because of group velocity dispersion (GVD) and the nonlinearity. This equation can be solved by using the inverse scattering method and the solution of this equation is the soliton which is reported by Zakharov and Shabat in 1971. In fact the NLSE has many solutions for each integer value of $N = \gamma P_0(t_0)^2/\beta_2$. When $N = 1$, the phase modulation due to GVD and the self-phase modulation which is represented as the right hand side term in the Eq. 2.12, can cancel each other perfectly if β_2 and γ have different signs. Considering the case for the silica fiber, γ is always positive, so β_2 should have the negative sign to have a perfect phase cancelation. As a result of this, Eq. 2.12 has a soliton solution and it propagates the nonlinear medium without changing its shape. This is the fundamental solution of the NLSE and referred as the fundamental soliton. Since the fundamental soliton preserves its shape during the propagation inside an anomalously dispersive fiber ($\beta_2 < 0$), a soliton is a good candidate for pulses in mode-locked fiber lasers.

The passive pulse propagation in an optical fiber can be modeled by the NLSE, but fiber lasers have components which cannot be modeled by several phase modulations in the NLSE such as a gain with the limited bandwidth and a saturable absorber. These components cannot modulate phase, but they cause the amplitude modulation in the time and the frequency domain. These terms can be added to the NLSE to count the amplitude modulation effects in a laser cavity. Then the resulting differential equation is called as a cubic Ginzburg-Landau equation (CGLE);

$$\frac{\partial A}{\partial z} = gA + (\frac{1}{\Omega} - 1\frac{D}{2})\frac{\partial^2 A}{\partial t^2} + (\alpha + i\gamma)|A|^2 A \tag{2.13}$$

where g is the net gain, which is the combination of the gain from the gain fiber and the loss due to the output coupling. Ω is referred as the spectral amplitude modulation such as the gain bandwidth or the intracavity spectral filter. α is the cubic intensity dependent amplitude modulation which is related to the saturable absorber. The solution of the Eq. 2.13 does not provide any information about the intracavity pulse evolution, yet the qualitative trend of the lasers with a strong evolution can be predicted. The solution of the CGLE

can be categorized as a dissipative soliton. Allthough parts of the dissipative solitons structure experience gain and loss of energy A dissipative soliton is a localized structures and it can exists for an extended period of time [75]. Since the dissipative processes (spectral filtering and saturable absorption) in the Eq. 2.13 are essential to form stable pulses in the fiber cavity, the solution of a fiber laser system can be categorized as dissipative solitons. In contrast, when the dissipative processes are not so important for the laser pulse shaping (i.e. soliton and DM soliton fiber lasers), the solutions of the lasers are closer to the solitons in conservative (Hamiltonian) systems. Due to its strong dissipative nature of the ANDi fiber laser, the pulse generated in the ANDi fiber laser definitely shows the features of dissipative solitons. In fact, the pulse generated in the ANDi fiber laser resemble the solution of a cubic-quintic Ginzburg- Landau equation (CQGLE) which is a modified version of the Eq. 2.13 [76].

2.3 Pulsed Operation

The bandwidth of the laser gain medium limits the range of wavelengths which amplification can occur inside the optical cavity for any specific laser. When the light is propagating inside the optical cavity, certain wavelengths which constitute the propagated light within the cavity, experienced amplification if they are within the gain bandwidth of the laser and the light forms a standing wave whereby those amplified wavelengths. This effect is observed when an integer number of half wavelengths of the light satisfy the boundary conditions and fits within the cavity length. Normally, thousands of wave maximas occur in the optical cavity for each standing wave, since each standing wave must have a specific wavelength. If there is more than one standing wave within the cavity, then each standing wave or referred to as a longitudinal mode of the cavity are separated by a fixed amount of frequency separation which is determined by the cavity length. This frequency separation can be found by dividing the speed of light by twice the cavity length. The number of longitudinal modes depends on the wavelength/frequency bandwidth of the laser gain medium. If there are more than one longitudinal modes inside the gain cavity, then those modes cannot be

distinguishable if spectrum analyzer is not used to analyze the beam because they are all in the same direction and their wavelengths are so similar.

Generally, when the laser emits a continuous wave light, then those modes will oscillate independently of each other with random phases relative to each other. Therefore the sum of electromagnetic fields of these modes inside the cavity will be noise-like and fluctuations are observed in the intensity because of the interference between modes. However, manipulating the phases of modes and obtaining a more useful output is possible by using a mode-locking technique.

If modes of a multi-mode laser has fixed and well-defined phase relationship, then those lasers are called mode-locked. After the phases are locked to each other by a well-defined relation, there will be a constructive interference at instant between the modes with a well defined function of time. As a result of this effect, the output will appear as a pulse.

We can describe the output of the multi-mode laser in the time domain as:

$$E(t) = \sum_{n}^{N} E_n e^{i(\omega_n t + \phi_n)} \tag{2.14}$$

where the sum is over all the electromagnetic fields of the cavity modes. E_n represents the amplitude of the n^{th} mode, ω_n and ϕ_n are for the frequency and the phase of the n^{th} respectively.

For the single mode laser cavity, Equation 2.14 contains only one term. If we want to make things more interesting, we can increase the gain bandwidth for covering more than one cavity modes. In this situation terms of Equation 2.14 increases, whereby the number of overlapping cavity modes. As a result of this, the output of such laser depends on the phase relationship between the overlapping cavity modes. If phases of each mode have a random relationship between each other, then in the time domain, we should observe that the laser is generating a continuous wave signal with a intensity noise (see Fig. 2.5 (a)). On the other hand, if we have a fixed phase relationship between the modes,

then the output of the laser changes dramatically as can be seen in Fig. 2.5 (c). With fixed phase relationship, these modes can constructively interfere with each other at the multiples of cavity round trip time, as they destructively interfere elsewhere. As a result of this process, pulses are created and the pulse duration is proportional to the number of phase locked cavity modes.

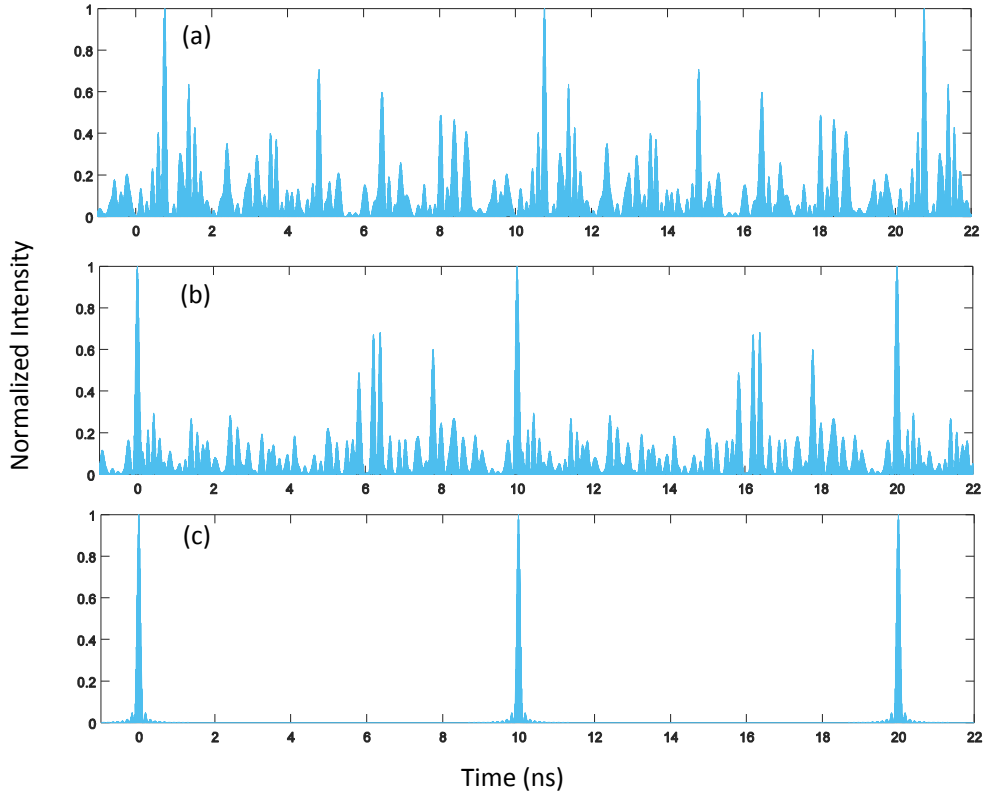

Figure 2.5: Simple simulation of mode-locking. The free spectral range of the cavity was arranged at 100 MHz and the cavity contained 80 modes. (a) The case for no phase relation, (b) partly phase coherent modes, and finally (c) all phase coherent modes. The MATLAB code for this simulation can be founded in Appendix A.

The most important question is how we obtain pulsed operation by achieving phase locking of the modes practically. In the following, we are focusing on the time domain rather than the frequency domain picture to understand mode-locking. We know that ultrashort pulses are created at one round trip time of the cavity by mode-locking. A pulsed operation is characterized by a periodic output signal, where each single pulse has a certain temporal intensity distribution, and

an intensity maximum. the intensity is zero between the pulses. To achieve this operation mode, one of the cavity elements needs to transmit the pulse peak intensity nearly without losses, while the lower intensity signal is damped between the pulse peaks. This cavity element is called as a saturable absorber. Real atoms were used as the first saturable absorbers. The basic principle of this mechanisim was based on the absorbing low intensity light the atoms while highly intensive light full excites the atoms and passes most of its photons through the medium. When we investigate the mode-lock process in the frequency domain, then we will need to a periodic amplitude modulation of the multi mode laser. If the period of modulation coincides with the round-trip time of the cavity, mode-locking occurs. In other words, in the frequency domain, every mode creates its own sidebands under a periodic amplitude modulation. The sidebands of any mode occur close to its neighboring modes. In turn, those sidebands can couple to their nearest neighboring modes which are leading to the phase-locking.

As will be seen in the next subsection, this behavior can be reproduced with optical processes without using any actual atomic absorption. There are two types of mode-locking: active mode-locking and passive mode-locking. In active mode-locking case, amplitude modulation can be applied by an active element inside the cavity which can be electrooptic modulator(EOM) or acousto optic modulator (AOM). In simple cases by neglecting group delay dispersion and self-phase modulation effects, the pulse duration can be calculated in the steady state by using Kuizenga-Siegman theory as $\tau_a = \sqrt[4]{D_g/M_s}$ [77]. This relation demonstrates that the pulse duration, which is achieved by active mode-locking decreases with the increasing modulation strength which is increasing with the square of the modulation frequency. This means that the system is limited because of external modulation which is dependent on the electronic speed. Therefore highest modulation can be obtained at the level of GHz and at that level pulse duration is typically in the range of picosecond. However if the pulse can modulate the absorption by its own, then the absorption modulation become large, which corresponds to shorter pulse duration. Therefore passive mode-locking technique can generate shorter pulse durations than active mode-locking technique. All of the studies using ultrafast pulses reported in this thesis utilize passive mode-locking.

A nice overview of active and passive mode-locking techniques are in reference cited [78].

2.3.1 Passive mode-locking

The general aspects of the mode-locking principle is discussed in the beginning of this section. Now this subsection is focused on passive mode-locking, which can be achieved by introducing a saturable absorber with suitable properties into the laser cavity. Saturable absorber can be categorized into two types: (i) artificial saturable absorbers using an all optical nonlinear process to generate pulses and (ii) real saturable absorbers include carbon nanotubes, semiconductor quantum wells.

Passive mode-locked lasers do not require any assistance from a modulator for achieving mode-locking. Therefore, the drawbacks of noise degradation which comes from the modulators are eliminated. This advantage makes them a good candidate for low noise and compact applications. In addition, only passive effects can provide a response time in the scale of femtosecond [79]. For that reason, passive mode locked laser have been exclusively used for generation of shorter pulse duration than the active mode-locking technique.

Saturable absorbers have been used as inducing a time dependent loss inside the cavity and their working principle is based on creating lower loss when they encounter with a more intense power. Therefore, continuous wave light experiences more loss than a pulse. Depending on the saturation properties of the cavity gain and saturable absorber, three different mode-locking mechanisms can be observed as is depicted in Fig. 2.6 .

A fast saturable absorber has a faster recovery time than the pulse duration (Fig. 2.6(a)). On the contrary, a slow saturable absorber restores slowly, which means that its recovery time is much longer that pulse duration (Fig. 2.6(b)) or it can be a slow saturable absorber with a saturable gain as is the case with dye lasers (Fig. 2.6(c)) [3].

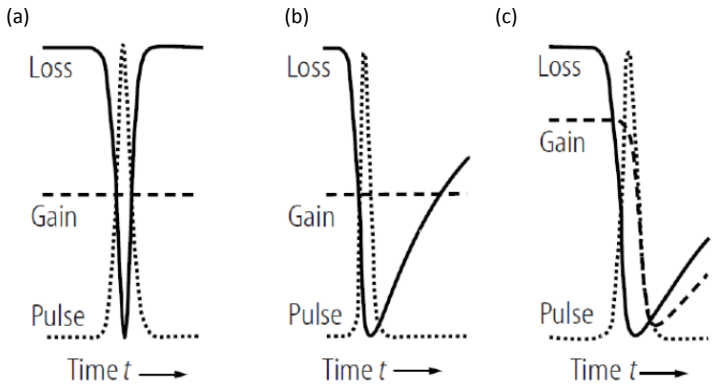

Figure 2.6: Temporal evolution of optical power and losses in a passively mode locked laser with (a) a fast saturable absorber, (b) a slow saturable absorber, (c) a slow saturable absorber and saturable gain [3].

In the case of a fast saturable absorber, instantaneous pulse intensity decides the state of the absorber. The leading and the trailing edges of the pulse experience the strong shaping. When the pulse duration is short enough than the recovery time of the saturable absorber (slow saturable absorber case), we encounter the opposite situation. This regime is preferred to the generation of ultrashort pulse durations instead of fast saturable absorbers because fast saturable absorbers are limited for pulse durations below 100 fs.

As a first case for estimating the expected pulse duration, we can consider a case with a fast saturable absorber without the influence of Kerr nonlinearity and dispersion effects and we can ignore the gain saturation during a pulse as an assumption. This situation generally occurs in picosecond mode-locked lasers with SESAMs and its analytical results have been derived by Haus et. al. [80]. Although, these calculations are only valid for weak absorber saturation, numerical simulations proves that the expected pulse duration can be estimated for a fully saturated absorber as [81];

$$\tau \approx \frac{0.9}{\Delta f_g}\sqrt{g/\Delta R} \tag{2.15}$$

where Δf_g is for the FWHM (full width half maximum) of the gain bandwidth which is assumed as a Lorentzian shape. g indicates the power of the gain coefficient which equals to the overall cavity losses. ΔR is the modulation depth of the absorber. If ΔR increases, then the required gain (g) also increases. Therefore, the greater value of ΔR than optical cavity losses corespond to the less pulse shortening of the optical pulse. As a result of this situation, the pulse duration is limited on the order of $1/\Delta f_g$. On the other hand, we can increase the FWHM of the gain bandwidth and slightly reduce the pulse duration by imposing a Kerr nonlinearity within the cavity. However, due to the excessive nonlinear phase accumulation, the dynamics become unstable.

Longer pulse durations are obtained in the case of a slow saturable absorber and when the influence of dispersion and nonlinearity is ignored, the expected pulse duration can be calculated as [4] with;

$$\tau \approx \frac{1.07}{\Delta f_g}\sqrt{g/\Delta R} \tag{2.16}$$

Eq. 2.3 is very similar to the estimated pulse duration for fast saturable absorber, yet in this case, Kerr nonlinearity always makes pulses longer in contrast to the fast saturable absorber. The generated pulse duration can be shorter than the recovery time of the saturable absorber. At this time, two drawbacks arise: (i) instability and (ii) reduced pulse quality. In such cases, pulse quality degrades because a weak pedestal can grow behind the pulse. The pulse shortening mechanism for the slow absorber is totally different than the fast absorber mechanism. The leading edge of the pulse is attenuated by the absorber; but then if there is an enough amount of energy in the pulse, the absorber medium is bleached part in the propagation direction of the pulse. Therefore, the trailing part of the pulse passes through the medium more or less unchanged. This situation creates an asymmetry in time, with a faster leading edge and an unchanged trailing edge [4].

Self starting mode locking is also desirable goal as well as generating the shortest pulse duration. In this respect, a slow saturable absorber can be valid candidate due to having a lower saturation intensity which facilitating the mode-locking in the early phase of the operation.

In this thesis, the fiber laser systems were built for a material processing which is the most important application. Despite the practical advantages of fiber lasers, these systems are limited by the ablation rates and for exploiting the fully ablation effect, higher repetition rates are required. However, ultrafast fiber lasers are limited by the repetition rate to the order of 100 MHz or even lower. In the frame of this thesis, it was targeted to develop a laser source with a repetition rate beyond the limitations. Therefore, two different mode-locking techniques were exclusively realized by passive mode-locking based on the intensity dependant polarization evolution in optical fiber and the dissipative four wave mixing. Both mechanisms will be explained in the respective chapter 3 which also contains the experimental results.

Chapter 3

High Repetition Rate Fiber Oscillators

3.1 Motivation

Use of sub-picosecond laser pulses operating at low (Hz or kHz) repetition rates allows precise material removal in the non-thermal regime [38]. However, heat affected zone, which causes undesirable changes in the structure of the target material can occur during ultrafast pulse processing as a result of pulse-to-pulse accumulation of residual heat that is deposited around the border of the ablated region by each pulse [82]. While deposition of some residual heat by each pulse is unavoidable, a laser system operating at very high repetition rates can catch much of this heat before it can diffuse beyond the volume to be ablated by the next incoming pulse. This brings three interrelated advantages: Most of the residual heat left by the previous pulse has not yet diffused out of the volume to be ablated by the next pulse. Thus, each pulse targets an already hot volume, which lowers the required ablation energy and peak power. In addition, the quantity of residual heat is proportional to the pulse energy, thus reducing the magnitude of the problem to be solved. Finally and most importantly, much of this already minimized residual heat is then carried away from the target during ablation

by the next pulse, drastically reducing the build-up of heat from pulse to pulse, considering to the heat conduction parameters of targets. Hence, the required repetition rate scales with the thermal conductivity of the target material and, in practice, ranges from tens to hundreds of MHz at a minimum.

Therefore, there is a growing interest in achieving high repetition rates in order to explore the advantages of a new ablation regime [1]. To this date, Fundamentally mode-locked ultrafast laser oscillators are limited to the order of 100 MHz or even lower repetition rates. Due to this limitation, researchers have been investigated and reported many different approaches like SESAM mode-locked semiconductor disk lasers operating in the range of GHz with the pulse duration of a few picosecond [83]. Despite their characteristic advantages for achieving a high repetition rate, these lasers are specialized solutions and lack of compactness, cost effectiveness and simplicity to operation.Therefore, all-fiber approach which fulfills all of these requirements has a great advantage for studiyng and realizing high repetition rate ultra-fast lasers. Femtosecond fiber lasers with a repetition rate of 1 GHz have been reported recently [84], yet further scaling up the repetition rate is extremely difficult due to inducing a sufficient nonlinearity. It is possible to scale up the repetition rate with the use of external passive cavities by multiplying the generated pulses externally but this approach is also quite complex [85]. Despite the high repetition rate characteristic of the fiber laser system, the researchers have to overcome the difficulty of complex design.

At the onset of this chapter, two different mode-locked oscillators have been demonstrated as seed sources for amplifier stages. We focus only on passive techniques for achieving high repetition rates. First laser was a fundamentally mode-locked Ytterbium fiber laser with a repetition rate of 100 MHz which was limited due to the cavity lengths. The repetition rates of hundreds of MHz are sufficient for achieving an efficient ablation process for various materials [18, 45]. Considering the technologically important materials like silicon, the thermal relaxation times can be measured as in the range of nanosecond, which corresponds to the repetition rate of GHz range for fully exploiting the ablation cooling effect. Towards this goal, we focus on another related technique, so called dissipative four wave mixing (DFWM), which is an excellent candidate for reaching the

range of GHz repetition rate and mode-locking can be achieved either with an overall anomalous or normal cavity dispersion. Therefore, the second laser was constructed based on the dissipative four wave mixing principle operating at a repetition rate of around 100 GHz at the wavelength of 1.5 μm. After fully understanding the mode-locking principle of DFWM then whose knowhow will be transferred at of around the wavelength range of 2 μm which is a crucial especially for tissue processing.

3.2 Fundamentally Mode-Locked 100 MHz Ytterbium Fiber Laser

In recent years, there has been an extensive trend in research activities that focus on developing ultrashort pulsed fiber laser sources because a large variety of applications like pulsed laser deposition [86], nonlinear microscopy [87], tissue processing [88], precision micro-machining [89] require shorter pulse durations, broad signal bandwidths and high peak powers. These applications have a great potential for scientific and industrial applications and they require cheap, compact, user friendly and robust laser sources. Fiber lasers can potentially fulfill all of these requirements. Therefore, a mode-locked Yb-doped fiber oscillator is described in the following section and this oscillator was used as a seed source for burst amplifier, which is explained in Chapter 4. Note that the results presented in this chapter were published in [90].

3.2.1 Principles of mode-locking by nonlinear polarization evolution

Additive pulse mode-locking through nonlinear polarization rotation has been used for generating stable pulses in fiber lasers [80, 91]. The experimental design contains a unidirectional cavity with two polarization controllers and a polarizer placed between polarization controllers. Mode-lock is achieved by using an

intensity dependent change in the state of polarization inside an optical cavity. The polarization state of a pulse evolves nonlinearly during the propagation inside a birefringent fiber because of the combination of self phase modulation [27] and cross phase modulation [27] and they induce phase shifts imposed on the two orthogonal polarization components. The polarization state of the pulse is nonuniform because the nonlinear phase shift is intensity dependent. The first polarization controller right before the polarizer is adjusted for forcing the polarization to be a linear in the central part of the pulse that the polarizing beam splitter allows the central intense part pass but blocks the low intensity wings. This effect is identical to that produced by a fast saturable absorber. Depending on the orientation of the polarization controllers, stable and passive mode-locking operation can be obtained.

Several distinct mode-locked regimes can be utilized according to their pulse evolution regimes such as soliton, streched pulse, dispersion managed, similariton, all normal dispersion (ANDi) and soliton-similariton. Among these we preferred to use ANDi laser to use as a seed source. ANDi fiber laser is a kind of new approach to pulse shaping based on spectral filtering of a highly chirped pulse. This laser design only consists of cavity elements with normal dispersion and there is no dispersion control in the cavity, so the extra spectral filtering becomes necessary to compensate the spectral broadening caused by the Kerr nonlinearity [76]. Spectral filtering also shortens the highly chirped pulse in the time domain. Highest pulse energies are obtained by ANDi lasers since the nonlinearity can be kept low due to long pulse duration. Therefore, we adapted an ANDi laser to the amplifier part which is described in Chapter 4.

3.2.2 Experimental setup

In this part, we report scaling the fundamental repetition rate of an Yb-fiber oscillator up to 100 MHz. We preferred Yb-fiber as a gain medium, because Yb-doped gain medium which emits 1 μm wavelength range provides the highest gain per length among available fibers in the commercial realm. It allows operation

with pump wavelengths very close to the signal wavelength which provides an opportunity to enhance the power handling capabilities. From an application point of view, material processing is the one of the most important applications of fiber lasers, which requires μJ energy levels at high repetition rates in order to scale up the processing speed. Therefore Yb-doped fiber lasers can fulfill all of these requirements. The first is the development of Yb-doped fiber oscillator for generating pulses and the second is building amplifier parts for increasing the pulse energy as preserving the pulse duration. However, increasing the repetition rate of these lasers is hampered due to the physical size of the components within the cavity in practice and threshold power for initiating passive mode-locking from the more fundamental point of view. Nevertheless, we have adapted an ANDi (all normal dispersion) laser as the seed source in this study due to its simplicity and robustness, similar in architecture to [92, 93] and tried to scaling the fundamental repetition rate up to 100 MHz, which is high enough to benefit from increased ablation efficiency [41] as working principle was mentioned briefly in the previous subsection.

The cavity setup can be seen in Fig. 3.1. The length of the light path inside the fiber and the air corresponded to 184 cm and 23 cm respectively for this configuration (see Fig. 3.1). With this parameters, the repetition rate of the oscillator coincided to 100 MHz.

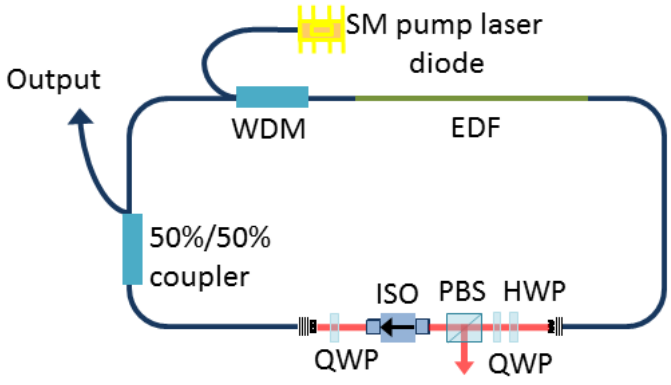

Figure 3.1: Schematic of oscillator operating at the repetition rate of 100 MHz. QWP: Quarter waveplate; HWP: Half waveplate; PBS: Polarisation beam splitter; ISO: Isolator.

The gain fiber was located at the beginning of the fiber section with respect to the propagation direction for maximizing the nonlinear effects and it had 500 dB/m gain at 976 nm with a core/cladding diameter of 6/125 μm and the length of 60 cm long based on the simulation results. Hence it was pumped with a single mode pump diode at the wavelength of 976 nm with a maximum output power of 300 mW. A wavelength division multiplexer (WDM) was used for spatially overlapping the pump wavelength of 976 nm and signal wavelength of 1030 nm which was created by the stimulated emission inside of the cavity.

Free space section of the oscillator was approximately 23 cm and it comprised two pieces of quater waveplates, one piece of half waveplate and a polarizing beam splitter cube for fulfilling the requirement of fast saturable absorber to obtain nonlinear polarization evolution. A bulk isolator was implemented to force the unidirectional operation. An interference filter with 10 nm bandwidth was placed right after the polarizing beam splitter cube for cutting the temporal wings of the heavily chirped pulse in the time domain and assisting the saturable absorber.

3.2.3 Experimental results

Self-starting mode-locking was achieved easily by adjusting the waveplates and the laser produced a stable pulse train with the repetition rate of 100 MHz which corresponded to a pulse energy of 0.13 nJ. The increasing the repetition rate of the laser cavity has consequences like a higher mode locking power threshold because of the shorter fiber segment resulting in a saturable absorption with a smaller amplitude modulation. Therefore, the repetition rate was chosen to be 100 MHz, which is high enough to benefit from efficient material processing [41] and is sufficient for mode-locking easily obtained by adjusting the wave plates.

Typical results for the output of the laser are shown in 3.2. The spectrum width was measured as 9 nm centered at 1034 nm with the pulse duration of 3.6 ps from the output port of the coupler. The output port of the coupler provided a direct fiber coupling the generated pulses from oscillator to the amplifier part and this situation eliminated the interruption of the seed signal because of misalignment.

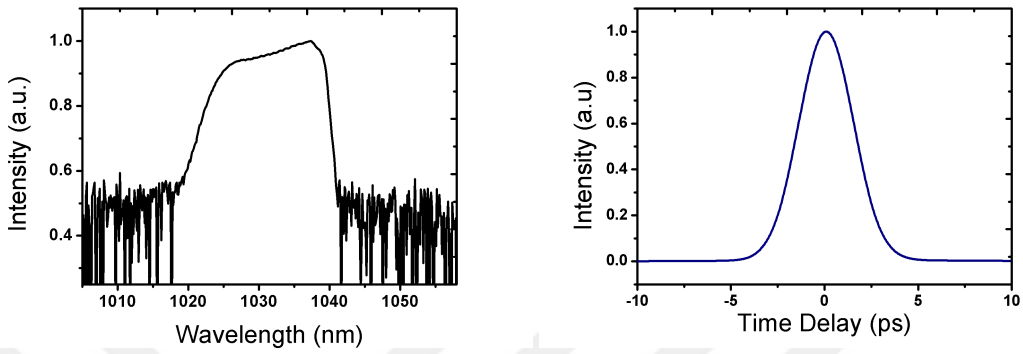

Figure 3.2: (a) Output spectrum of oscillator in a semi-log scale. (b) Measured autocorrelation trace of chirped pulses with a pulse duration of 3.6 ps from a output port 50/50 % coupler.

High average power and energy pulsed laser systems are built based on master oscillator power amplifier (MOPA) configuration. This configuration contains one oscillator part where low power pulses are formed and the amplifier part where peak power of the pulses is amplified. In this section, the oscillator part and the pulse formation are described and the following chapter provides the complete setup containing the amplifier part which is working based on burst mode operation.

3.3 Intracavity Dissipative Four-Wave Mixing at Different Dispersion Regimes of an Ultrafast Fiber Laser

We investigated a system which generates the ultrahigh repetition rate stable pulse trains for different dispersion regimes. The dissipative four wave mixing (DFWM) is the main mechanism for the formation of the remarkably stable train of pulses at different dispersion regimes. We achieved a stable mode-locked operation at the repetition rate of 100 GHz which is fixed by the free spectral range of an employed Fabry-Perot filter.

3.3.1 Principles of mode locking by dissipative four wave mixing

Ultrafast fiber lasers offer an attractive platform for implementing high repetition rate pulse sources besides their high gain coefficient and wide operating wavelength ranges [84]. In recent years, generating stable pulses with the range of high repetition rates beyond the limitations of active and passive mode locking hase gain a great interest [61]. As a result of this interest, Yoshida *et. al.* introduced a pioneering approach for the formation of stable ultrahigh repetition rate pulse trains as resulting from modulation instability by employing a Fabry-Perot filter inside the main cavity and they obtained a train of pulses with a repetition rate of 115-GHz [94]. Sylvestre *et. al.* have discovered that the DFWM process has a significant role in the pulse generation process rather than modulation instability [95]. The basic principle of DFWM is that there is only two frequencies inside the bandwidth of the gain medium which experience the net gain and after that they transfer their energies to their higher order harmonics by four wave mixing (FWM). After the reinterpretation of Yoshida's approach by Sylvestre, Peccianti *et al.* have recently reported a mode-locked oscillator with a stable ultra high repetition rate by inserting a high-Q factor microring resonator for an optical element of either generating the nonlinearity or a Fabry-Perot filter into the fiber cavity called as filter-driven four wave mixing (F-D FWM) [96]. To date, researchs about DFWM are based on a fixed setup and achieving higher repetition rate. Despite the elegance of the pulse generation with high repetition rate based on DFWM technique, learning how to manage and compensate dispersion and nonlinear effects in the cavity is essential to ensure their stable operation. However, the pulse dynamics inside the laser cavity has not been fully understood and it requires more investigation especially the effects of the net cavity dispersion on the pulse evolution.

Pulse train generation can be achieved by using a mixing of two frequencies in the case of different fibers [97, 98]. In what follows, Teixeiro *et. al.* proposed a new scheme for passive mode-locking by investigating an extended Ginzburg-Landau equation [99]. They used a limited gain bandwidth and there were two

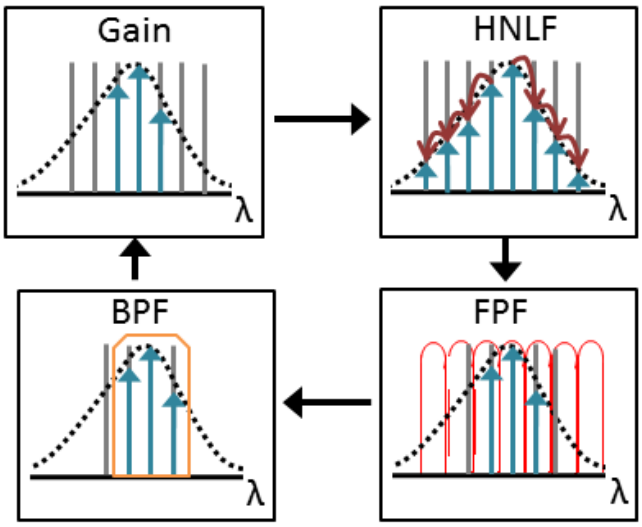

Figure 3.3: The schematic of mode-locking principle. HNLF: Highly nonlinear fiber; FPF: Fabry-Perot filter; BPF: Bandpass filter.

symetrical peaks inside this bandwidth which actually experienced the gain. After calculations, they obtained unchirped pulse train with the high repetition rate.Therefore, the nonlinear fiber behaved like a self starting component that depends only on the fiber parameters. In this mechanism, only two frequencies are important for the pulse generation which one is near the maximum point of the gain and they transmits their energy by wave mixing [27] to its harmonics, which is outside of the gain.

The mode-locking principle is illustrated in Fig. 3.3. The Fabry-Perot filter contributed to the four wave mixing generation, as the energy in the cavity was selectively confined in the longitudinal modes of the Fabry-Perot filter. The selected modes, then transferred their energy to higher idler modes from four wave mixing with the help of dispersion shifted highly nonlinear fiber. Due to the nature of the four wave mixing process [27] all modes had a constant phase relationship and as a consequence of Fourier theorem, a train of pulses with a repetition rate given by FSR of the Fabry-Perot filter was created.

3.3.2 Experimental setup

The schematic diagram of the laser setup is shown in Fig. 3.4. The resonator consisted of a 1.88 m of Er-doped fiber, an isolator for preventing the unidirection propagation, two polarization controllers, 50 m of highly nonlinear dispersion shifted fiber with the nonlinear coefficient of 11 $1/Wkm$ for inducing strong nonlinear effect. Normal dispersion fiber was used as a delay line with different lengths for scanning the net cavity dispersion both the anomalous and normal dispersion regimes.

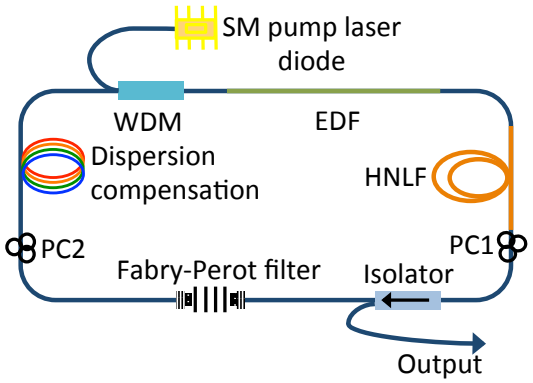

Figure 3.4: Setup of the high repetition rate fiber oscillator. WDM, wavelength divisionmultiplexer; EDF, erbium-doped fiber; PC1 and PC2, polarization cotroller 1 and 2; HNLF, highly nonlinear fiber with zero dispersion at 1550 nm.

The net dispersion of the laser cavity (β_{net}) was varied from $0.041 \pm 0.002 ps^2$ to $-0.02 \pm 0.004 ps^2$ according to the lenght of the normal dispersion fiber. The FPF was constructed by employing a fiber coupled u-bench, stacked glass substrates and a bandpass filter. The number of stacked glass substrates increased the finesse of the FPF based on serial connected etalons. The thickness of the glass substrates was fixed to 1.2 mm which corresponds to the FSR of 100 GHz.

3.3.3 Experimental results

To investigate the dependence of the laser performance on the FPF, we conducted experiments, one without FPF for revisiting the concept of modulation instability and the other with FPF. We gained experimental results of laser operation with different values of net cavity dispersion for both cases. Additionaly, we investigated the effect of bandwidth filter to the pulse generation.

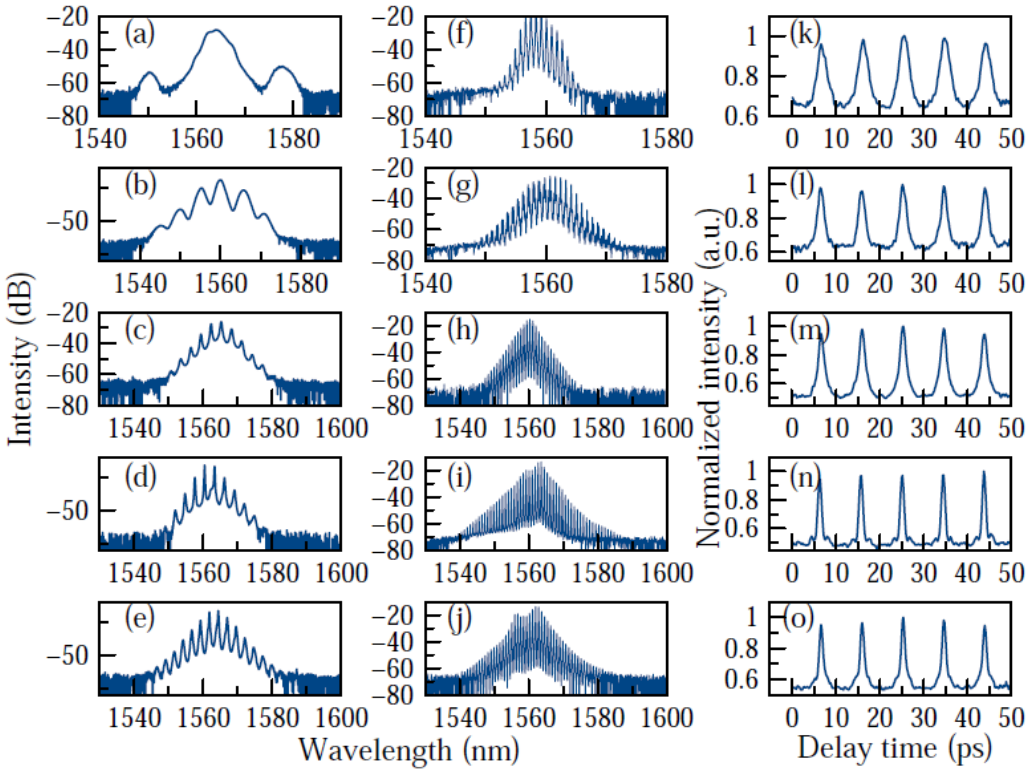

Figure 3.5: Left-hand column (a-e), output spectra of the laser operating at (a) 0.041, (b) 0.02, (c) 0.009, (d) -0.009 and (e) -0.02 ps^2 of net dispersion values without the Fabry-Perot filter. Middle column (f-j), output spectra of the laser with the Fabry Perot filter at corresponding net dispersion values respectively. Right-hand column (k-o), autocorrelation traces of the laser at the same net dispersion values with a 100 GHz repetion rate for all regimes.

Fig. 3.5 (a)-(e) depicted the spectra of MI states which are characterized by a degenerate pump, whereas the spectra in our results exhibit a odd number of

peaks [95]. However, due to the nature of MI, it was difficult to generate a stable train of pulses with a well defined repetition rate. Stability of the system was achieved by insertion of a FPF inside the cavity. By doing so, self-starting pulse trains were always obtained in the cavity by adjusting the settings of PCs and the average output power was around 38 mW. Fig. 3.5 (f)-(j) show the output spectra of the cavity with the FPF for different values of β_{net}. The corresponding autocorrelation traces as shown in Fig. 3.5 (k)-(o), demonstrate that the laser produced equidistant pulses with 10 ps of temporal spacing for all cases with pulse durations of 1.69, 1.55, 1.13, 0.78 and 0.77 ps respectively which were related to choice of β_{net} and depended on the shape of the mode-locked spectrum. According to Fig. 3.5 (f)-(j), we defined the value of CW component/peak pulse intensity in the autocorrelation and for the case of without bandpass filter this value was on the level around 50 %. When the bandpass filter installed into the cavity, it played a crucial role for ensuring that only a few central modes experience a possitive gain and thus introduced dissipation to the cavity. Then the prevented energy can be stored in the lower harmonics instead of transfering to the higher harmonics for preserving the fix phase relationship between the modes [100]. As a result of this, the value of CW component/peak pulse intensity reduced down to the level around 30 % with the constant pulse duration of 2.1 ps for all cases of dispersion values depending on the bandwidth of the bandpass filter (see Fig. 3.6).

DFWM is a particularly attractive method because mode-locking can be achieved either with an anomalous or normal cavity dispersion, leading to the generation of bright or dark pulse trains, respectively [95]. In our case, there was an interplay between the mode-locking states of nonlinear polarization evolution and dissipative four wave mixing in a complex manner. The laser initially started in continuous wave operation however, once the gain of Erbium-doped fiber was increased above a certain value it mode-locked by a nonlinear polarization evolution which is described in Section 3.2.1. The FPF contributed to the FWM generation, as the energy in the cavity was selectively confined in the longitudinal modes of the FPF. As a result of four wave mixing, the phases of the generated longitudinal modes were locked and chirped-free pulses were formed [99]. The

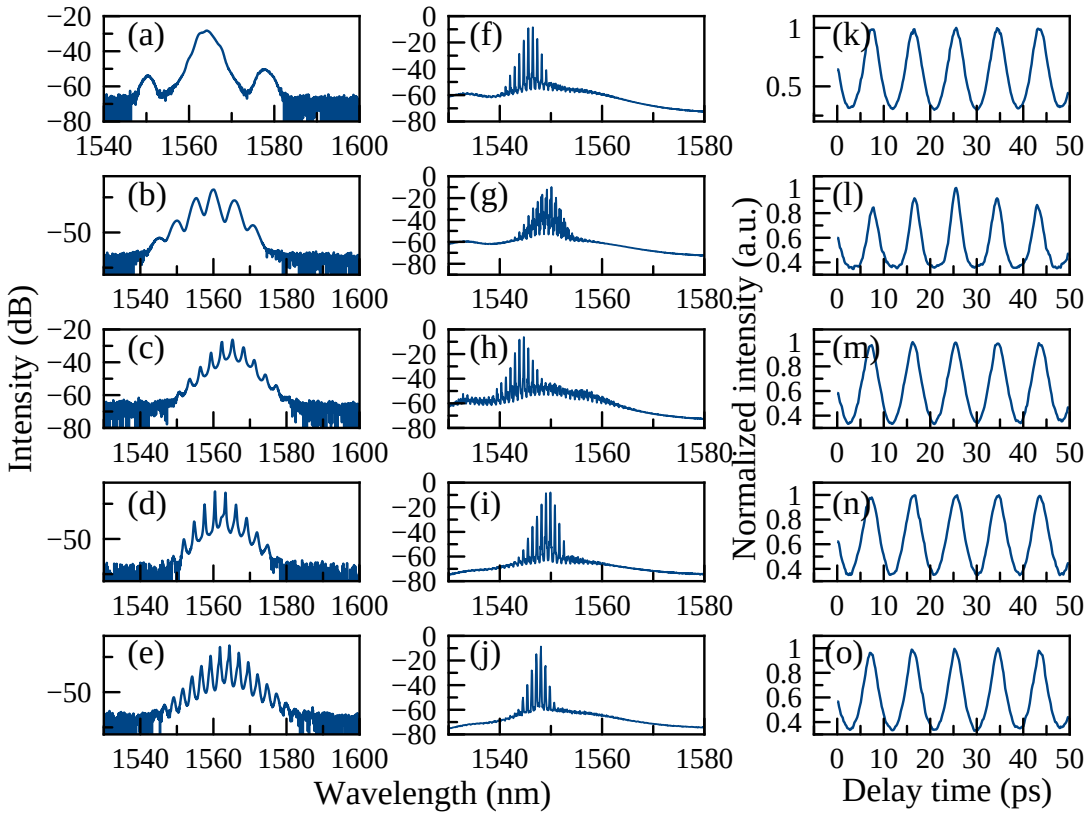

Figure 3.6: Left-hand column (a-e), output spectra of the laser operating at (a) 0.041, (b) 0.02, (c) 0.009, (d) -0.009 and (e) -0.02 ps^2 of net dispersion values without the Fabry-Perot filter. Middle column (f-j), output spectra of the laser with the Fabry Perot filter and a bandpass filter at corresponding net dispersion values respectively. Right-hand column (k-o), autocorrelation traces of the laser at the same net dispersion values with a 100 GHz repetion rate for all regimes.

repetition rate of the laser was depending o the frequency separation between two longitudinal modes and in our case this corresponds to FSR of the FPF. Therefore, the repetition rate of the laser setup was fixed for the corresponding values of net cavity dispersion.

Comparisons with and without FPF were provided which revealed differences in the features of the dynamics of pulse formation in the cavity. The laser was not only capable of operating in the state which is referred to DFWM. By extracting the FPF, a mixed operation state was existent, where MI and NPE were observed and interacting in a complex manner. With the help of FPF, the optical spectrum of the pulses was modulated periodically and DFWM dominated the operation state. Hence, we obtained a stable train of pulses with the repetition rate of 100 GHz, corresponding to FSR of Fabry-Perot filter for normal, anomalous and around zero dispersion regimes based on DFWM. This technique is useful because a stable pulse oscillation with a constant repetition rate can be obtained without any complexity for all dispersion regimes.

3.4 Conclusion

In conclusion, we have demonstrated the mode-locked fiber laser oscillators having the high repetition rates. The first system produced pulses at 1μm wavelength and capable of generating an uncompressed pulse duration of 3.6 ps with a repetition rate of 100 MHz with a pulse energy of 0.13 nJ. The mode-lock was obtained by nonlinear polarization evolution and we preferred ANDi laser as a seed source [76]. It has already been shown that, application of pulsed-burst at tens of MHz pulse repetition frequencies on target materials increase the ablation efficiency, using the advantage of residual heat left behind by the previous pulse [41, 44]. The results on increased ablation efficiency for hundreds of MHz in-burst repetition frequencies for copper targets and heat-free ablation of human dentine and mouse brain samples have also been demonstrated by our group [101]. In addition to these results, Kerse *et. al.* has proven that the delivery of ultrafast pulses at an order of magnitude lower pulse energies with repetition rates

of tens of MHz provides an order of magnitude better ablation efficiency without any sign of heat affected zone compared to the case of delivering pulses at higher energies with repetition rates in the order of 1 – 100 kHz [102]. Therefore, to utilize this seed source to a processing platform for exploiting ablation with ultrafast pulses, mode-locked Yb-doped signal, which was explained in the first section of this chapter with the repetition rate of MHz range was amplified to desired pulse energies, explained in the following chapter.

Despite the efficient ablation process for most materials at the range MHz repetition rate, materials with high thermal conductivity require higher repetition rates. Since building such high repetition rate mode-locked lasers have practical limitations, a promising way is to use DFWM with the help of Fabry-Perot filter. The Fabry-Perot filter modulated the optical spectrum, which was already mode-locked by NPE periodically assisted by highly nonlinear fiber which induced the four-wave mixing process. As a result of this, we obtained a stable train of pulses with the repetition rate of 100 GHz, which corresponded to the free spectral range of the Fabry-Perot filter. The laser setup was designed with the Er-doped fiber emitting a wavelength of 1.5 μm for fully understanding the mode-locking principles, yet this method can be applied to normal, anomalous and zero dispersion regimes without any complexity. This technique is a promising way for generating ultra high repetition rate pulses without any complexity. It can vastly expand with state of the art developments across the entire spectrum of industry to medical. Therefore, our aim is that develop a laser system operating around 2 μm for tissue processing applications and our motivation is to apply the ablation cooling idea to tissue processing in the high water absorption wavelength region and obtain a system that holds a big potential for laser surgery. For this goal, we are planning to transfer our knowledge on ultra-high repetition mode-locked oscillator and the burst mode amplifier, which are described in this chapter and next chapter respectively to the fiber laser system operating around 2 μm where tissue interaction.

To utilize these seed sources to a processing platform for exploiting ablation with ultrafast pulses, mode-locked signals, which were explained in this chapter with the repetition rate of MHz and GHz ranges should be amplified to desired

pulse energies. The design and construction of the mode-locked resonator seed sources to be assisted by mode-locking mechanism should be followed by the construction of the amplifier system which are explained in the following chapters for achieving desired pulse energies.

Chapter 4

Development of High Power Continuously-Pumped Burst-Mode Amplifiers

4.1 Motivation

Research on developing ultrafast pulse amplification using fibre amplifiers is proceeding at a high pace for use in applications areas in a research laboratory and also the outside of the research laboratory [20, 23]. Nonlinear optics, metrology and spectroscopy have been reported as well known application areas for ultrafast lasers. In addition, the ultrafast laser can be used as an advanced tool for material processing with greatly reduced or absent heat effects [103] such as fabrication of miniaturized devices, precision micromachining of variety of materials, self-assembly techniques as well as highly controlled surface texturing through ultrafast laser material processing [104], pulsed laser deposition of extremely high quality films [105].

It is commonly accepted that the use of ultrashort pulses allows operation in the so-called non-thermal regime, which indicates major benefits in processing of

various materials, including biological tissue with a high precision and uniformity which cannot be obtained with conventional lasers [105]. To observe the benefit of ultrashort pulses the pulse duration should be shorter than the electron-phonon thermal coupling time of the material for preventing heat distribution around the interaction region [38]. Despite the material's diffusion time, single pulse with a pulse duration less than 10 ps is enough for exploiting non-thermal ablation [82, 106]. Based on this idea, it is assumed that each laser pulse is targetted on the material, cannot cause of any heat generation and as a result of this situation, precise material processing is achieved [54].

The main obstacle to a wide spread of laser micromachining, despite their unique possibilities, is the fabrication efficiency. The way of increasing the efficiency of micromachining process is to increase the repetition rate and average power of laser system. Already, fiber lasers producing 1 MHz repetition rate pulses with 10s of Watt average power and microjoule energies have led to scaling up the processing speed [41, 42]. However the high repetition rate pulsed systems are currently limited by the average power for achieving high pulse energies which are necessary for obtaining an ablation process. This situation can be considered by the hypothetical scenario of generating 10 mJ pulses at a continuous repetition rate of 100 kHz. Such system requires the output power of 1 kW which is challenging in the manner of an excessive heat accumulation on the laser system and output power of the pump diodes which also causes a large amount of thermal loading. Therefore, the repetition rate of high pulse energy systems are limited. However, there are many applications that require high pulse energies at a high repetition rate, but this requirement is only for a certain amount of pulses not a long time. One way of circumventing this issue, the new concepts have been investigated to contribute to this tremendous development and the pulse burst concept is one of that ones, which allows the system to operate at high repetition rates over a short period of time while keeping the average power low [41, 44]. This concept has been a very interesting and until recently underappreciated technique to generate bursts of high repetition rate pulses at a lower overall repetition rate. In this fashion, the thermal load on the system is kept within manageable limits.

Burst-mode lasers based on solid-state lasers have been around for a much longer time but these lasers typically have pulse duration in the picoseconds and in some cases even in the nanosecond range. Examples of this kind of lasers were demonstrated in the studies by Lempert, et al., and the amplifiers used in these systems were based on Nd:YAG [107–109], generating pulses with 9 Hz and 50 kHz repetition rate and pulse energies varying between 10 and 400 mJ, and the number of pulses in a burst could be adjusted between 1 to 99. This reported system utilizes a low averge power of order of 100 mW master oscillator and pulses are sliced into bursts with the help of acousto-optic deflector [110]. These systems were used in niche applications such as observation of gas flow in aeronautical system, burning and exploding process diagnostics. Additionaly. this mode of operation possesses a great potential for ultrafast material processing. The ablation efficiency per pulse has been predicted to scale up by almost an order of magnitude with burst-mode lasers system when we compare the material processing results of uniformly spaced pulsed laser systems of same energy, duration and power. The feeling in the optics community is increasingly that the burst mode is the method of choice for material processing but due to a lack of suitable laser sources, this opportunity remains largely unexplored to date. Therefore this unique technique can be combined with fiber laser technology due to their reliability, high beam quality, relatively compact size, lower cost and flexibility.

Recently, Kalaycıoğlu, et al. have demonstrated the first high-energy burst-mode fiber lasers and developed it [2,42,47]. Breitkopf, et al. reported on a lower-repetition-rate, higher-burst-energy fiber laser [43]. These lasers were pumped with laser diodes pulsing in synchrony to the bursts to minimize amplified spontaneous emission (ASE), which complicates the laser setup. Thus, it is important both scientifically and in terms of practical development of ultrafast burst-mode lasers to better understand and characterize the limitations from ASE buildup between bursts.

Additionally, we report a detailed characterization of the burst repetition rate and associated ASE generation that can be achieved under continuous pumping. ASE generation is monitored directly in a special time-gating measurement setup. Other methods for ASE measurement have been reported in [111]. To measure

ASE, the laser system generates bursts with average power of 50 W. The bursts contain between 10 and 125 pulses with burst repetition rates between 1 MHz and 80 kHz, while keeping the average pulse energy at 5 μJ. We find that pulsed pumping is not required at burst repetition rates above 200 kHz to maintain an ASE ratio of less than 2%. Based on these results, we scaled output power up to 145 W for 1MHz burst repetition rates comprises of 10 pulses inside the burst. The pulse duration is estimated to be 13 ps, representing $\sim$ 1.5-fold and 1.9-fold in average power and peak power respectively, as well as a 30% reduction in pulse duration, compared to our previous results [112]. The estimated ASE ratio is less than 2%. These constitute the highest average power results for any ultrafast burst-mode laser, to the best of our knowledge. In this study Dr. Parviz Elahi helped in the construction of the experimental setup and measurement. Note that the most of the results presented in this chapter were published in [48].

4.2 Experimental Setup

The experimental setup is summarized in Fig. 4.1 and is similar to that described in [112]. A five-stage laser amplifier is seeded from a mode-locked fiber oscillator [76] which is described in Chapter 3, supplying 13-mW, 3.6 ps-long chirped pulses through its fiber port. The spectral bandwidth is 9 nm, centered at 1034 nm. The repetition rate of the oscillator is chosen to be 100 MHz, which is high enough to benefit from increased efficiency during burst mode operation [41]. A fiber-coupled acousto-optic modulator (AOM) is used to impress the envelope that defines the pulse bursts. Each burst contains an adjustable number of pulses, ranging from 10 to 125 pulses per burst, depending on the burst repetition rate, such that individual pulse energy is kept constant.

The pulses are first stretched to 41 ps in a 120 m-long standard singlemode fiber. The first and second amplifier stages comprise core-pumped Yb-doped fibers (40 cm-long with 500 dB/m absorption at 976 nm and 15 cm-long with 1200 dB/m absorption at 976 nm, respectively) with 6 μm core diameter. A single pump diode is used, splitting its output by 30% and 70% to pump the first and

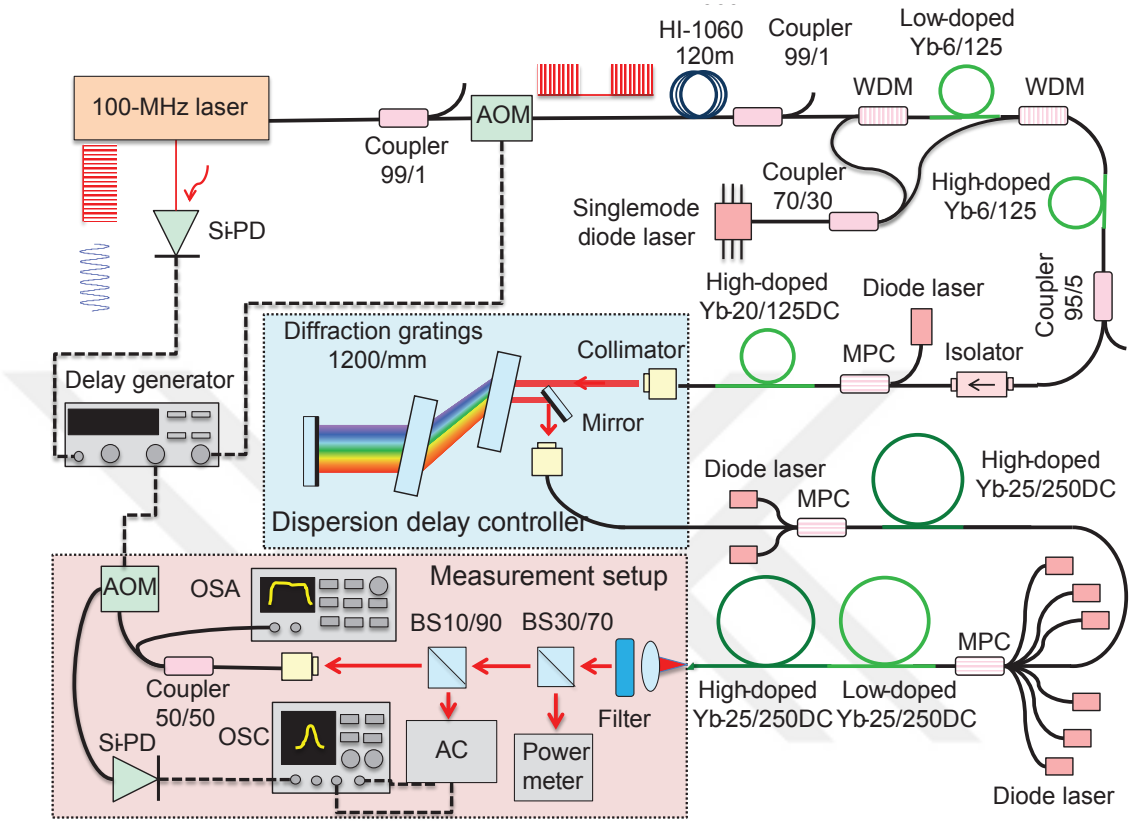

Figure 4.1: Schematic diagram of the setup: AOM, acousto-optic modulator; WDM, wavelength-division multiplexer; MPC, multiple pump-signal combiner; Si-PD, silicon photodetector; AC, autocorrelator; OSA, optical spectrum analyser; OSC, oscilloscope.

second stages, respectively. Amplified power is 150 mW. This is followed by an inline isolator. The third state comprises 140 cm-long double-clad (DC) Yb-fiber with 20 μm core diameter and 125 μm for cladding diameter (29 dB/m cladding absorption at 976 nm). A 2-port pump-signal combiner is used to launch pump power of 16 W from a multimode diode laser, which is temperature stabilized to operate at 976 nm. The signal pump is thus increased to 11 W. Given the complexity of grating-based compression beyond roughly 100 W of average power, we implemented the approach demonstrated in [112], namely, negatively prechirping the pulses prior to launching into the power amplifier, generating chirped, $\sim$10 ps pulses directly. Coupling to the power amplifier is achieved with a fiber-pigtailed collimator with a lead fiber of 20 μm-core diameter. The high-power amplifier is the most challenging part of the system. Nonlinear effects and thermal effects

limiting the achievable peak and average power levels, respectively. Therefore, we designed this section as composed of two power amplifier stages. The first power amplifier and fourth overall stage of the setup utilizes a 2.8 m-long DC Yb-doped fiber with 25 μm core diameter and 250 μm cladding diameter with 6.5 dB/m cladding absorption at 976 nm. This stage is pumped by two 25-W pump diodes (Oclaro, Inc.), delivered through a 2-port pump-signal combiner. The launched signal is 3.8 W and the output power is 34 W. The measured slope efficiency is 70%. The fifth and final stage implements discrete doping management using a combination of high-doped and low-doped fibers [90]. The low-doped first section is the same fiber as used in stage four with identical core and cladding diameters. The high-doped fiber has also same core and cladding diameters, but its cladding absorption is 10.8 dB/m. The relative lengths of the two fibers (1 m of low-doped fiber, followed by 2.7 m of high-doped fiber) were determined, first coarsely through numerical simulations, using an improved version of the model reported in [93] and fine-tuned experimentally. A 6-port pump-signal combined is used to deliver pump light from 6 diode lasers. The diodes are temperature stabilized to operate around 976 nm.

4.3 Results and Discussion

In order to optimize the laser system, it is essential to understand the limitations on burst mode parameters arising from the laser dynamics, including the important limitation imposed by ASE generation. Full exploitation of the benefits of ultrafast burst mode, repetition rate of the pulses comprising the bursts should be at least tens of MHz, and preferably higher. Then, due to the short durations between pulses inside the burst, pumping during bursts cannot substantially repopulate the upper state of the gain medium, which implies that virtually all of the pump energy has to be delivered and stored in the gain medium during the intermission between subsequent bursts. ASE generation between the bursts not only depletes the population inversion, reducing gain available for the bursts upon their arrival, but only generates spurious quasi-CW emission, filling in between the bursts. The ASE generated in the first amplifier is amplified in the the next

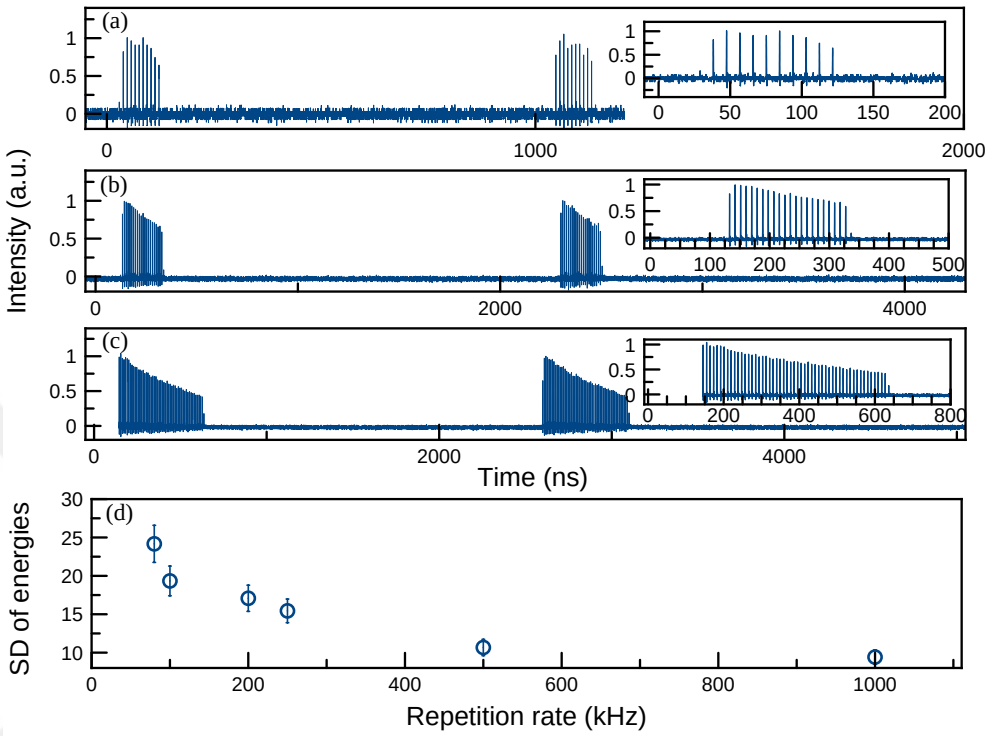

Figure 4.2: Measured temporal profile of the pulse burst at 50 W output power. Inset: Close-up showing the pulse train at repetition rates of (a) 1 MHz, (b) 500 kHz, and (c) 200 kHz. (d) Standard deviation (SD) of pulse energies within the pulse bursts as a function of burst repetition rate measured at 50 W.

stage and generate

The ASE is amplified proportional to the gain generated in the first amplifier addition, since ASE is generated in both directions, the component of ASE propagating in the direction opposite to that of the pulses can cause heating-related damage to earlier amplifier stages or lead to detrimental giant pulse formation. These possibilities have particularly serious implications in the kHz repetition rates, unless synchronously pulsed pumping is utilized. Furthermore, with increasing stored energies, the first few pulses of the burst deplete much of the gain at low repetition rates, leading to significant energy variations across the burst [42].

4.3.1 Burst characterisation and ASE measurement

To characterize burst dynamic, we implemented a measurement setup which enables to investigate the detailed system characteristics simultaneously, as well as measure ASE content directly in the time domain as first described in [113]. Fig.4.1 depicts the measurement setup. Output of the gain fiber of final amplifier stage is angle-cleaved to prevent back reflected light from getting coupled back into the core. After collimating the beam, residual pump light is filtered out with a dichroic mirror. For autocorrelation and optical spectrum measurements, power is decreased with a non-polarizing 70%/30% beam splitter. The larger portion is sent to a powermeter for continuous monitoring. The smaller portion is passed through a second, non-polarizing, 90%/10% beam splitter, sending its smaller portion to the autocorrelator and larger portion to a fiber collimator. The fiber coupled light is further split into two equal arms with a fiber coupler for optical spectrum and ASE measurements. The ASE measurements are performed by passing the light through a second AOM, which is gated with the negative of the signal applied to the first AOM with a properly adjusted delay. The resulting action is to drop the burst signal, such that any (ASE) signal between the bursts is easily detectable with a sensitive powermeter. Further details can be found in [113]. Since presence of substantial amount of ASE signal not only limits the achievable pulse energy, but can also lead to catastrophic damage to the laser system, utmost care was taken during the ASE characterizations. As a precaution, the output power was limited to 50 W. In order to rule out any indirect influence of nonlinear effects on the ASE measurements, which could occur due to, e.g., changes in efficiency due to Raman-induced red-shifting of the spectrum, the (average) pulse energy was kept constant (5μJ). This was achieved by adjusting the number of pulses per burst between 10 and 125, corresponding to burst energies ranging from 50 μJ to 625 μJ and burst repetition rates ranging from 1 MHz to 80 kHz, respectively.

Pulse burst generated from the power amplifier is shown in Fig.4.2(a) for 1 MHz burst repetition rate which corresponds to 10 pulses inside the one burst.

Depletion of the gain during the burst is considerable, which results in significant variation in pulse energy across the burst. Especially, when the time delay between two burst is increased (burst repetition rate is decreased), the variation becomes significant (Fig.4.2(b-c)). Fig.4.2(d) shows the measured pulse energy variation across the burst for different burst repetition rates. This variation can be compensated for by preshaping the burst envelope [42] at the cost of increased complexity in control electronics. However, at burst repetition rates above 500 kHz, standard deviation of the pulse energy within a burst is less than $\sim 10\%$ (Fig. 2(d)). In this work, preshaping is not utilized for sake of simplicity. Experimental measurements demonstrate that ASE between bursts rises sharply for burst repetition rates below 200 kHz (Fig.4.3(a)). However, the fractional amount of energy within ASE signal remains in the range of a benign and acceptable level of 1% for burst repetition rates of 200 kHz and higher.

4.3.2 Optimization and power scaling

Having determined the dependence of ASE levels and pulse-to-pulse energy variations as a function of the burst repetition rate, we have optimized the system for high-power operation. At a burst repetition rate of 1 MHz, ASE ceases to be a limiting factor. The laser system generates 100 ns-long bursts, containing 10 pulses each. The maximum average power is 145 W, limited by available pump power and the slope efficiency is $\sim 70\%$ (Fig.4.4(a)).

Fig.4.4(b) shows measured optical spectrum for 50, 100 and 145 W output power, corresponding to 5, 10 and 14.5 μJ of individual pulse energies, respectively. As the pulse energy is increased, four-wave mixing and intra-pulse Raman scattering lead to spectral broadening and red-shifting substantially beyond the gain bandwidth.

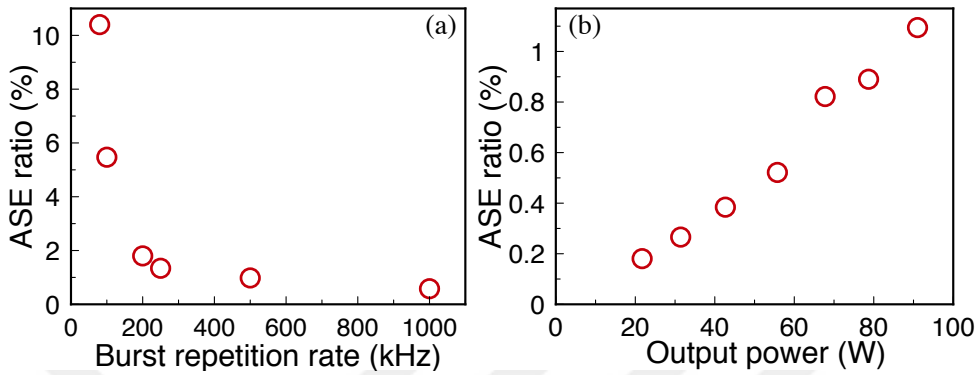

Figure 4.3: (a) Measured ASE/output power ratio as a function of burst repetition rate at 50 W output. (b) Measured ASE/output power ratio versus output power, for which the burst repetition rate was kept at 1 MHz.

However, gain narrowing ultimately limits the spectral width to 70 nm. The average energy for the pulses within the burst is 14.5 μJ. The variation of energy in the burst is calculated to be 9 %. The measured autocorrelation signal is presented in Fig.4.4(c), fitted by a Lorentzian pulse intensity shape, which provides a better fit than the commonly used Gaussian shape. The inferred full-width half-maximum (FWHM) pulse duration is 12.8 ps. We also used the PICASO algorithm [114] to fit the measured autocorrelation and optical spectrum with an arbitrary spectral phase profile, from which the inferred FWHM pulse duration was 12 ps. We note that while this retrieval procedure (Fig.4.4(d)), cannot predict the pulse shape accurately it gives an arguably more reliable estimate of the pulse duration than simply fitting the autocorrelation trace with a fixed pulse shape, but the results should be considered as a replacement for proper pulse retrieval.

At the highest powers of 145 W, the estimated nonlinear phase shift in the last stage of amplification is about 180 π. The resulting spectral evolution is dominated by Raman scattering, as evidenced by the asymmetric growth of the spectrum towards longer wavelengths. However, there is a complex interplay between Raman scattering, SPM and higher-order dispersion, while soliton-like effects that typically underlie similar spectral enchancements do not play a significant role since the fibers have normal dispersion and the pulses are positively chirped in the regions where nonlinearity is the strongest. As to be expected, there

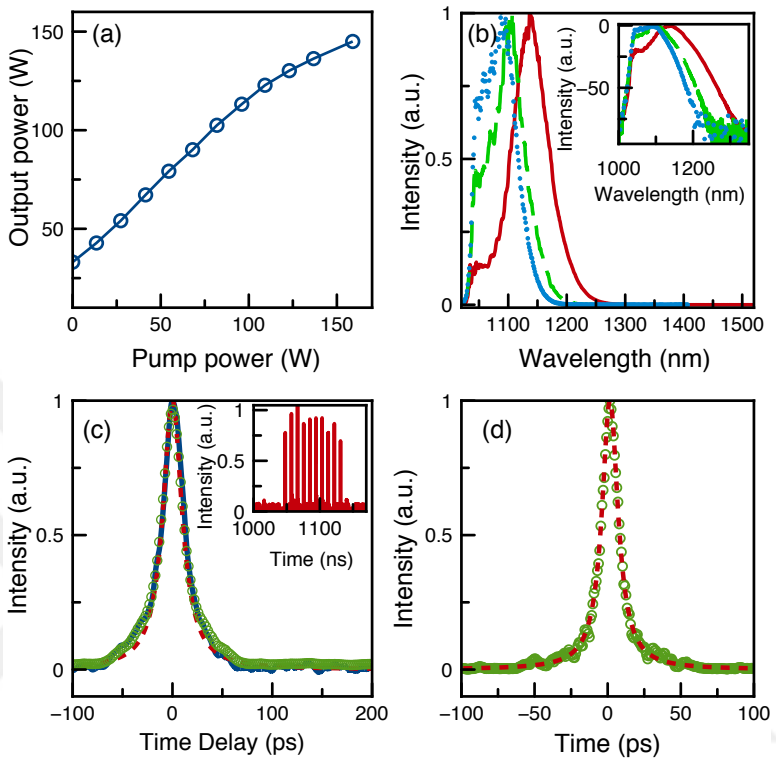

Figure 4.4: (a) Measured output power versus pump power. (b) Measured output spectra in burst mode operation at output powers of 50 W (blue-dotted line), 100 W (green-dashed line) and 145 W (red-solid line) shown as linear and inset: semi-log plots. (c) Measured intensity autocorrelation at 145 W of output power (blue-solid line) along with retrieved autocorrelation trace obtained using PICASO (green circles) and Lorentzian fit (red-dashed line). Inset: pulse train in one burst from power amplifier at 145 W output power. (d) Retrieved pulse shape (green circles) and Lorentzian fit (red-dashed line) with FWHM of 12 ps.

is a trade-off between nonlinear spectral reshaping and pulse duration, similar to the results in [90]. If the launched pulses are more heavily chirped, nonlinear effects are reduced, but this results in longer pulses. For shorter launched pulse durations, nonlinear spectral broadening leads to additional dispersive stretching. Thus, the pulse duration becomes clamped. However, by implementing doping management with a third segment with even higher doping level (increasing the gain/length), gain filtering can be exploited to reduce pulse durations to sub-10 ps.

4.4 Conclusion

In conclusion, we have carried out systemic investigations of ASE generation for a burst-mode fiber laser system using a direct, time-domain measurement system. Our results indicate that pulsed pumping employed in [2, 42, 47] is not required as long as bursts are repeated at 200 kHz or higher for 50-W operation, which allows for substantial simplification of the setup. Even lower repetition rates would be possible at lower average powers. In addition, preshaping of the pulse energies within the burst in order to decrease the pulse-to-pulse energy variations is not needed for high burst repetition rate cases, which further simplifies the electronics of the setup. Based on this analysis, we have constructed a fiber laser system operating in the burst mode regime. This laser system generates 145-W, 13-ps pulses directly from fiber, which is the highest average power for ultrafast burst-mode operation, to the best of our knowledge.

Chapter 5

Development of Fiber Lasers in the Range Between 1.9 μm and 2 μm

5.1 Motivation

Laser usage in medical applications is rapidly spreading due to the advantages lasers have in diagnostic and surgical procedures. Especially surgical operations using lasers with no blloddy cutting procedures, redue greatly after-effects such as travma and healing period. The fact that the high water content in soft tissues causes high absorbtion at the wavelength of 1.95 m makes lasers working at this wavelength and higher wavelengths where water absorption peaks exist important for surgical applications. Currently, mostly solidstate lasers operating at these wavelengths are used; however, they are generally bulky, have low energy efficiency ve high cost and hence these factors limit their usage. Especially in the last two years, development effort for the development of continuous-wave (CW) and long-pulsed thulium-doped fiber (Tm-fiber) lasers have intensified. This is presenting a similar technologIc development to the case of Er-fiber lasers in the 1990s and Yb-fiber lasers in the 2000s. Tm-fiber lasers are able to operate at 1.95

m where the water (highly present in tissue) has an absorption peak.

Successful tissue processing with laser emitting the wavelength of 2 μm has been demonstrated by using thulium or holmium ions as a gain medium inside of the laser system [115, 116]. Medical operations in which tissue is removed with these lasers are suffer from a low speed of process. The speed of removal process can be simply increased by scaling up the repetition rate of the laser system. At the same time, the average power is also increased, resulting in significant collateral tissue damage due to pulse to pulse accumulated the residual heat. Both of these problems can be overcame through the implementation of groups of high-repetition-rate pulses, or bursts at the wavelength range of 2 μm. Nevertheless, utilization of Tm and Ho doped systems to burst-mode operation are newly emerging technology and have been historically limited due to technological developments compared to the other gain mediums like Ytterbium. Therefore, the main motivation of this chapter is to develop core technologies for applying the burst-mode operation to the laser system operating at the wavelength of 2 μm.

The optical spectrum of Ho-doped fiber lasers exhibit at the longest wavelengths of all the silica based fiber lasers (2- 2.15 μm) with high efficiency and excellent beam quality. Therefore they are promising sources for the above application and also their emission corresponds to the transparency window of atmosphere (2-2.3 μm), which provides advantages over the Tm-doped fiber lasers. However, Ho-doped fiber lasers fall behind Tm-doped lasers, owing to problems associated with the pumping schemes, which is a drawback from a practical point of view and one way of the overcome this drawback is using Tm-doped fiber laser as a pump source. Tm-doped fiber lasers appear to be well-suited for the generation of high signal power with a low quantum defect and subsequently a low thermal load due to an efficient cross-relaxation process which occurs in heavly doped thulium fibers, making such fibers suitable for high power lasers [117].

Compared to conventional fiber the pump absorption is increased due to larger overlap between pump distribution and the active core and coupling the pump into the core of the fiber provides a better overlap than coupling into the cladding

of the fiber resulting shorter fiber length and better efficiency. However, coupling the pump into the core of the fiber requires the pump source with a high quality. In-band pumping of Ho-doped fiber lasers with a mature Tm fiber laser by using a core-pumping technique is an attractive route to high output power and high pulse energy in the 2 μm. Consequently, this chapter consists of two main sections. The first section contains construction of spectrally combined Tm-doped fiber lasers as a pump source. We demonstrate an all-fiber integrated four-wavelength Tm-doped fiber laser with an output power of 38 W by using the spectral beam combining method. Tthe laser oscillators which are spectrally combined by using in-house-made WDMs are operating at the wavelengths of 1920, 1949, 1997 and 2030 nm. This work is published in [118]. Secondly, building a Ho-doped fiber amplifier by using a dual-wavelength pumping scheme is explained. The power combined system was employed as high brightness pump source for Holmium doped fiber laser. We obtain an average power of 9 W from Ho-doped fiber amplifier resulted in an efficiency of 68 % with the dual wavelength pumping concept.

5.2 Single-Mode Spectral Beam Combining of High Power Tm-Doped Fiber Lasers with WDM Cascades

The development of high power fiber lasers have gained a great interest in recent years as a result of the practicality of these lasers, having a possibility to generate high power with excellent beam quality which is ideal for applications throughout research and industry. New directions are constantly being pursued to utilize the capabilities of this technology and one of these directions involves extending the emission wavelength further into the infrared range which will be needed for numerous existing and future applications [119–121]. Although the variety of rare-earth ions transitions and host materials have been tested for fiber laser emission in different wavelength regimes, a clear decrease of output power

is observed at [122] as plotting the maximum obtainable continuous wave output power of fiber lasers as a function of emitted wavelength. The primary reason of the decreasing behavior of obtainable continuous wave output power is the growth in the quantum defect at longer wavelengths when the system is pumped with the traditional pump sources for silicate glass fiber lasers which are emitting light in the near infrared region close to 1 μm. Although the excellent cooling properties of optical fibers help to reduce the problem of high quantum defect, which creates heat that becomes an increasing fraction of the absorbed pump power, development of high power pump sources at longer wavelengths and selecting more appropriate laser transitions can be effectively used as diminishing the effects of high quantum defect and improving the laser output performance.

Therefore, scaling fiber lasers to high average output power is of current interest, especially at longer wavelengths [123–127]. Despite the easier engineering at longer wavelengths, owing to a number of scaling factors, scaling the power of single mode fiber lasers is still limited by optical or thermal damage of the fiber including thermal aberrations and nonlinear effects. Fundamental nonlinear and thermal limitations on the power scaling of fiber lasers which can be encountered by a single laser source are leading researchers into beam combining schemes to achieve higher continuous wave laser power. The goal of beam combining cannot simply be to increase the power, but to preserve the beam quality for applications in which high intensity is required on the target. The beam combination method will provide a path to even higher power with an excellent beam quality by using developed methods [128, 129] with the help of increasing the power level within each individual laser unit.

A common approach for beam combining is to use a wavelength selective element to combine spectrally non-overlapping laser sources. To date, almost all wavelengths combination schemes operate at 1 μm and 1.5 μm bands. Also, despite the technical difficulties, beam combining of Thulium sources was demonstrated recently [130]. However, the beam quality of the laser sources degraded completely due to the use of combiners employing multimode fibers. Spectral beam combining utilizing single mode WDMs is a promising approach, as the high beam quality of the laser building blocks is maintained [131, 132].

In the following experiments, spectral beam combining of four thulium-doped fiber oscillators by using a highly efficient in-house-made WDM cascade is investigated. The combining section consists of three WDMs, while two of them were used for combining oscillators with a small wavelength separation of 30 nm, a third one was used to combine both wavelength sub-groups. Our approach enables further power scaling by increasing the output power of the distinct laser oscillators and by increasing the number of channels of the cascaded combination scheme of WDMs.

5.2.1 Experimental setup

The experimental design used in this work is sketched in Fig. 5.1. It contains the fiber laser sources and the spectral-beam combination scheme. As laser sources, four identical continuous wave oscillators were employed each emitting narrow line-width signals at distinct wavelengths, which are 1920 nm, 1949 nm, 1996 nm, and 2030 nm with a respective output power of 7 W, 17 W, 20 W and 13 W as shown in Fig. 5.1. The cavity was entirely fiber-integrated, including pump delivery, which rendered the system misalignment free. The linear laser cavity comprised of a section of double-clad Tm-doped fiber, high-reflecting fiber Bragg grating (FBG), a low-reflecting FBG acting as output coupler, a pump combiner with a fiber integrated pump port and pump diode up to a power of 50 W. The schematic of the experimental setup is shown in 5.1.

5.2.2 Experimental results

5.2.2.1 Manufacturing & Characterization of WDMs

The WDMs were fabricated by the fused biconical taper technique. Single mode fibers (SMF28) were employed, which had an NA of approximately 0.13 around a wavelength of 2 μm. While the core diameter was 10 μm, the cladding diameter was 125 μm. The used fibers had a pure silica cladding. We simulated light

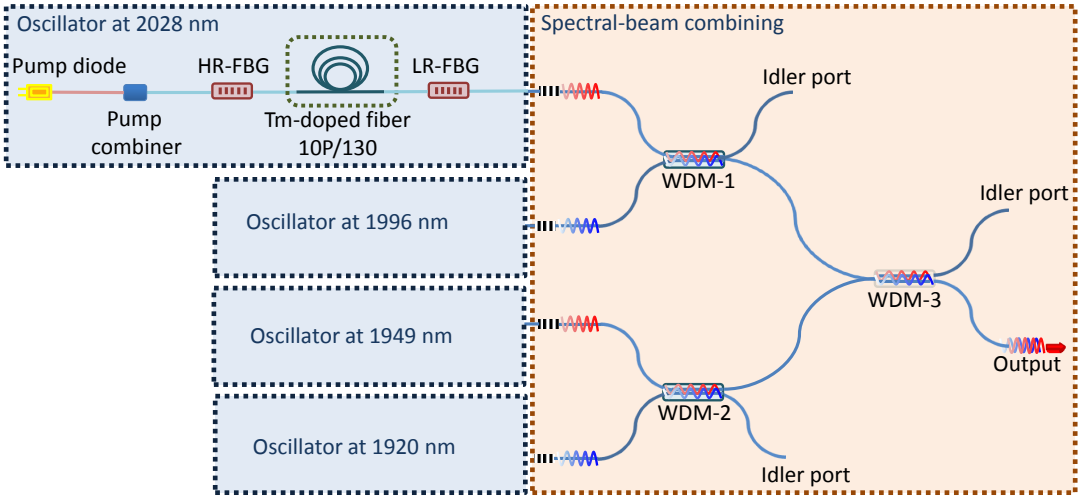

Figure 5.1: One of the continuous-wave fiber oscillator setups for spectral-beam combining and the schematic diagram of the spectral beam-combining setup. HR-FBG: High reflective fiber-Bragg grating, LR-FBG: Low reflective fiber-Bragg grating, WDM:Wavelength-division multiplexer (WDM1 for combination of 1996 & 2030 nm, WDM2 for combination of 1920 & 1949 nm).

propagation in the fused fiber couplers with our FFT-based BPM algorithm [133, 134]. The optical fibers were heated with a torch between two twisted points to cause the core-cladding mode coupling. Schematic deployment of the setup for the fabrication is explained in detail by Birks et. al. [135]. We modified the manufacturing process to achieve efficient WDMs for coupling the wavelengths of 1920, 1949, 1996 and 2030 nm. The developed WDMs were characterized in terms of insertion losses of the respective branches of the WDMs and spectral dependence of the coupling ratio.

5.2.2.2 Fiber Laser Oscillators

High power fiber lasers contained three major technologies, such as high quality active fibers, passive fiber components which can handle high power and bright pump diodes. For the laser sources, two types of fibers were used. First one was the pump fiber which has 105/125 μm core/cladding diameters. The other fiber type has 10/125 μm DC core/cladding diameters for single mode operation. The

active medium consisted of 5 meters of Tm-doped fiber with a peak absorption of 3 dB/m at the wavelength of 793 nm. The length of the gain fiber was optimized by maximum attainable signal power. For pumping the system, fiber coupled pump diodes from DILAS were used emitting at a wavelength of 793 nm. One of the FBGs was highly reflecting (99 %) and the other one was partially reflecting (10 %). Their reflectivity became maximum at their central wavelength which determined the operation wavelength of the system with a bandwidth of 1 nm. The combining scheme foresaw a combination into two subgroups with in-house-made WDM1 and WDM2 (1920/1949 nm and 1996/2030 nm). These subgroups were then multiplexed with in-house-made WDM3. With the aim of demonstrating a power combination employing the WDM cascade, we developed four identical Tm-doped single-mode continuous wave fiber lasers with an output power of 7 W, 17 W, 20 W and 13 W respectively, operating at central wavelengths of 1920 nm, 1949 nm, 1996 nm, and 2030 nm which are defined as L1, L2, L3 and L4 for being easily understood the Fig. 5.2. The slope efficiency of each system was $> 40\%$ demonstrating cross relaxation [117].

5.2.2.3 Combining two wavelengths with WDM1 & WDM2

The laser outputs were spliced to the in-house-made WDMs for spatially overlapping the beams with differing wavelengths as shown in Fig. 5.1. First, the behavior of the WDM1 and WDM2 was investigated by measuring the output power at the respective signal ports separately. The measured output power as a function of the launched signal power for both of the lasers was shown in Fig. 5.2(c-d) respectively. The coupling efficiencies of the WDMs were higher than 84 % and the same for both wavelength groups. The spectra of combined wavelength groups were depicted in the Fig. 5.2(a-b) for WDM1 and WDM2 respectively. For the spectral measurement setup, we used a neutral density filter to attenuate the output power of the WDMs due to the average power limitation of the spectrum analyser. Although, this filter had a particularly weak wavelength dependence, it caused the modifications of the spectral intensities during the spectral measurements of the maximum signal output power.

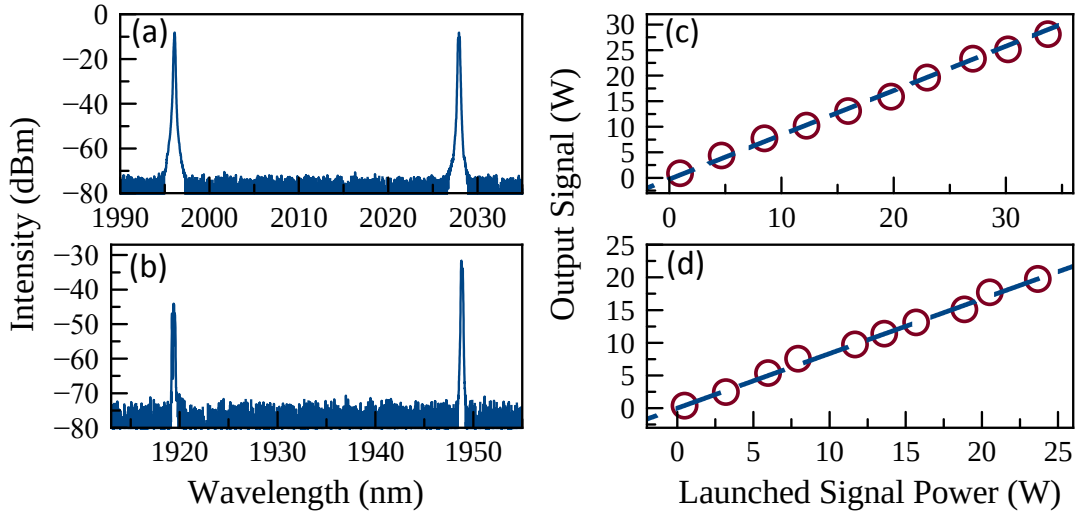

Figure 5.2: Spectral measurement at the signal port of (a) WDM2 and (b) WDM1. Combined optical power at the signal output port of the WDM2 (c) and WDM1 (d) with respect to the launched signal power for L3-L4 nm and L1-L2.

5.2.2.4 Combining four wavelengths with WDM3

The setup for the combination of the two subgroups by the WDM3 is shown in Fig. 5.1. The spectrum measured at the output port of the WDM3 is shown in Fig. 5.3(a) and the combined laser power with respect to the launched signal power is depicted in Fig 5.3(b). From Fig. 5.3(a), it is obvious that all wavelengths were successfully coupled to a single output port. We achieved more than 38 W of output power at a total input power of 48 W, which results in a combining efficiency of 80 %. Two loss mechanisms can be identified for the combination of signals. The first one is the insertion loss of the WDMs and the second is caused by the coupling of the signal power to the idler port which can be observed as a slow fluctuation of signal power at the output port. The error bars in the Fig. 5.3(b) represent this fluctuation.

A power of almost 5 W was coupled to the idler port of WDM3 at the maximum signal power level, which corresponds to 10 % of the input power, and caused the degradation of the coupling efficiency. The overall combining efficiency can be calculated by dividing the output power to total input power to be around 69 %.

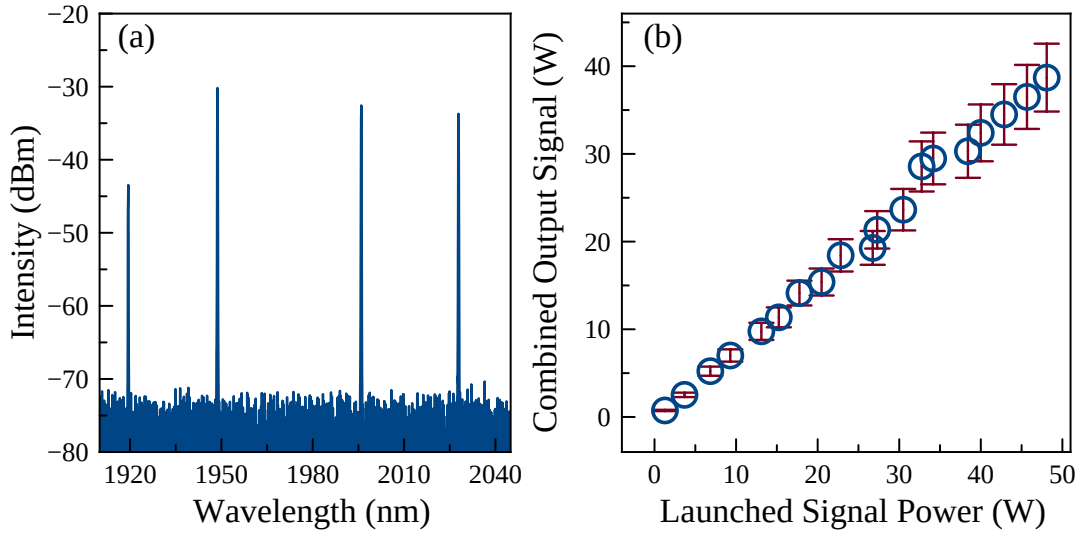

Figure 5.3: (a) Spectral power distribution at signal output port of WDM3. (b) Output power at signal output port of WDM3 with respect to input power.

5.2.3 Discussion

Spectral beam combining is an idea that historically has not received as much attention as coherent beam combining. However, interest in this technology is increasing rapidly, primarily because of the less demanding design requirements for building such systems and the high demand by applications which are not wavelength selective or which require the combination of distinct laser wavelengths. With our current implementation, we provide an all-fiber integrated design which is an alternative approach for obtaining not only flexibility and simplicity but also high output power with an excellent beam quality.

Due to the single mode fiber geometry most challenging are the onset of detrimental fiber nonlinearities like stimulated Brillouin scattering during the propagation of light after the oscillators in the fiber of the WDMs. In the weakly guiding approximation, the mode area of the lowest order mode scales as λ^2 where λ stands for the laser operating wavelength. This has a beneficial effect on the power scaling of fiber lasers at longer wavelengths. However, the drawback still arises from nonlinear effects that limit the maximum attainable output power after a threshold while maintaining the reliability for truly single mode high

power operation. For the suppression of these effects at the higher power levels, distributing the power between different wavelengths is a promising approach for increasing the maximum attainable truly single mode output power [136].

The cascading concept offers maximum efficiency for largest possible separation of the wavelength groups and smallest possible separation of wavelengths within respective groups. Therefore, scaling up this configuration to an even higher power can also be expected by increasing the power per channel and increasing the number of channels which is related with the number of WDMs being used in the cascade design. Improvements on further power scaling by including additional channels can be achieved by combining a smaller spectral separation which is limited by manufacturing parameters of WDMs. At the same time, the number of individual channels can be increased which is also related with largest possible separation of the wavelength groups inside the Tm-gain bandwidth of more than 100 nm around 1900 nm. Hence, a further scaling by additional and more powerful channels appears to be feasible in a straightforward manner.

5.2.4 Conclusion

In summary, we demonstrated all-fiber truly single mode power combination of Tm-doped fiber lasers employing a WDM cascade. By using fiber-Bragg gratings as highly reflective mirrors and output couplers, the distinct fiber lasers operated at wavelengths of 1920, 1949, 1996 and 2030 nm. The lasers were combined by using an in-house-made WDM cascade. The expected wavelength spacing can be specified by choosing FBG pairs with proper central wavelength and can be combined with changing the properties of the WDM. We achieved more than 38 W of output power from the signal port and the overall combining efficiency was measured to be 69 %. With a continuing improvement in high power fiber lasers and WDMs with high power handling capability, single mode operation at higher output power level can be achieved. This developed source offers excellent characteristics to serve as high brigthness pump in an Holmium doped fiber amplifier. in the next section the employment of such a spectrally combined source for core

pumping holmium doped fiber is investigated in detail.

5.3 Dual Wavelength Pumping Scheme For Resonantly Core-Pumped Holmium Doped Fiber Lasers

High power fiber lasers with an excellent beam quality are ideal for numerous applications throughout many scientific and technological fields despite the domination of solid state lasers. Recently demonstrated fiber lasers can match the performance of solid-state lasers albeit at one wavelength.The work is thus needed to extend their wavelength further into the infrared range, which will be needed for numerous existing and future applications such as remote sensing and biomedical applications [119, 120]. The resonantly pumped Ho-doped fiber lasers by a mature high brightness Tm-doped fiber laser is an attractive scheme to high output power and pulse energy with a low quantum defect and subsequently a low thermal load around the wavelength range of 2 μm.

Despite the easier engineering at longer wavelengths, owing to a number of scaling factors, scaling the power of resonantly pumped single mode Ho-doped fiber lasers has still drawbacks. Here two drawbacks remain, i.e., optical or thermal damage of the fiber including thermal aberrations, nonlinear effects and unsuitable properties of the conventional low index polymers for guiding the infrared light due to the strong absorption. Previously, the application of a spectral beam combining method based on a WDM cascade was demonstrated for building the high brightness and high average power pumping source that can be provided by combination of Tm-doped fiber lasers with different wavelengths and enables efficient scaling of Ho based amplifiers to high average powers based on core pumping technique [118]. Due to the single mode fiber geometry, the most challenging is the onset of detrimental fiber nonlinearities like stimulated Brillouin scattering (SBS) that limits the maximum attainable output power after a threshold while maintaining the reliability for truly single mode high power operations.

Therefore distributing the pump power of Tm-doped fiber lasers between different wavelengths as a pump source for a Ho-based amplifier based on WDM cascade design offers a promising approach for increasing the maximum attainable truly single mode output power by increasing a threshold of the nonlinear effects. Due to the nature of core pumping, the maximum pump absorption can be obtained from a strong overlap of pump wavelength with the Ho-doped fiber core. Introducing a cladding part as a buffer prevents the infrared absorption of low index acrylate polymers [137]. Therefore, this pumping scheme is suited to provide an efficient Holmium amplification with a shorter active fiber length compared to a cladding pumping technique. This scheme requires an accordingly shorter length of active fiber compared to a cladding pumped scheme. Therefore thermal loading has to be balanced with reduced fiber length.

5.3.1 Experimental setup

Here, a solution to facilitate heat dissipation and reduction of operating temperature in Ho-doped fibers by employing two pump wavelengths is presented. We propose a dual wavelengths pumping scheme in analogy to doping management to mitigate the thermal load on the active medium [90, 138].

In this scheme, we used two different pump wavelengths with different absorption coefficients of Holmium (see Fig. 5.4). The pump wavelength with low absorption coefficient ensures that the thermal load is reduced at the beginning of the active medium where the temperature impact is highest. Simultaneously, the second pump wavelength with a high absorption coefficient increases the absorption process to minimize the gain length and consequently to minimize the nonlinear effects. Therefore, the dual wavelengths pumping technique provides a significant advantage over conventional pumping schemes by suppressing thermal loading and nonlinear effects which are critical to any high power laser systems.

Tm-doped fiber lasers were demonstrated with high output power before [139]. In our work, we are using Tm-doped fiber lasers as a pump source with up to 20 W to make a proof of concept for the demonstration of temperature management

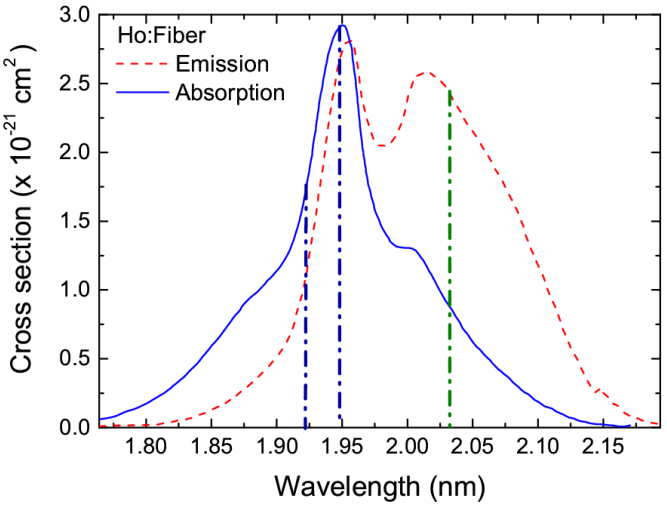

Figure 5.4: Absorption and emission cross section graph for Holmium fiber with respect to the wavelength. Blue dashed-dotted lines represent the wavelengths for pumping (1920 nm and 1950 nm) which are inside the absorption bandwidth of Holmium fiber with different cross section values. The green dashed-dotted line is the emission wavelength of Holmium at 2030 nm.

and power scaling of resonantly pumped Ho-doped fiber lasers by core pumping. The experimental setup is divided into three parts: (i) the fiber laser sources for pumps and signal, (ii) the spectral beam combination parts based on WDM cascade design and (iii) Ho-doped fiber amplifier as depicted in Fig. 5.5. As laser sources, two identical Thulium doped continuous wave oscillators are employed each emitting narrow line-width signals at distinct wavelengths, which are 1920 nm and 1949 nm with an output power of 8 W and 10 W respectively. Also we built a continuous wave Tm-doped oscillator with a wavelength of 2030 nm but we can use it for Ho-amplification as depicted in Fig. 5.4. All laser setups were combined with two WDMs, which have different specifications (WDM1: 1920 & 1950 nm, WDM2: 1920, 1950 & 2030 nm).

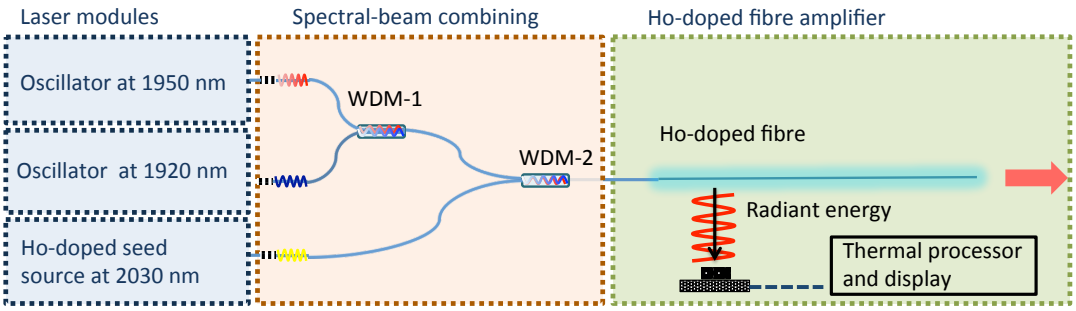

Figure 5.5: Continuous-wave fiber oscillator setups for spectral-beam combining, the schematic diagram of the spectral beam-combining setup and the Ho-doped fiber amplifier with a dual wavelength pumping scheme. WDM: Wavelength-division multiplexer (WDM1 for combination of 1920 & 1950 nm, WDM2 for combination of 1920,1950 and 2030 nm).

5.3.2 Experimental results

The outputs of Tm-doped fiber lasers were spliced to the in-house made WDM for spatially overlapping the beams with the wavelengths of 1920 nm and 1950 nm as shown in Fig. 5.5.

The measured output power of WDM1 as a function of the launched signal power coming from the Tm oscillators is shown in Fig. 5.6(b). We obtained an average power of 20 W in total as a pump source for the Ho-doped amplifier. The spectrum of the combined wavelength group is depicted in Fig. 5.6(a) for WDM1. Encouraged by theoretical investigation and experimental observation based on the doping management concept [90, 138], we have constructed the Ho-doped fiber amplifier that consisted of a gain length of 2 meters with the dual wavelengths pump source. Fig. 5.6(c-d) shows the measured power scaling behavior for individual pump wavelengths separately for observing the individual effects of the pump sources. We obtained an average power of 4.2 W and 5.3 W with an efficiency of 63 % and 65 %.

The amplified signal after the Ho-doped fiber pumped by two pump wavelengths is shown in Fig. 5.7. The spectrum of the combined beams is shown in Fig. 5.7(b) and the output power with respect to the combined pump power is

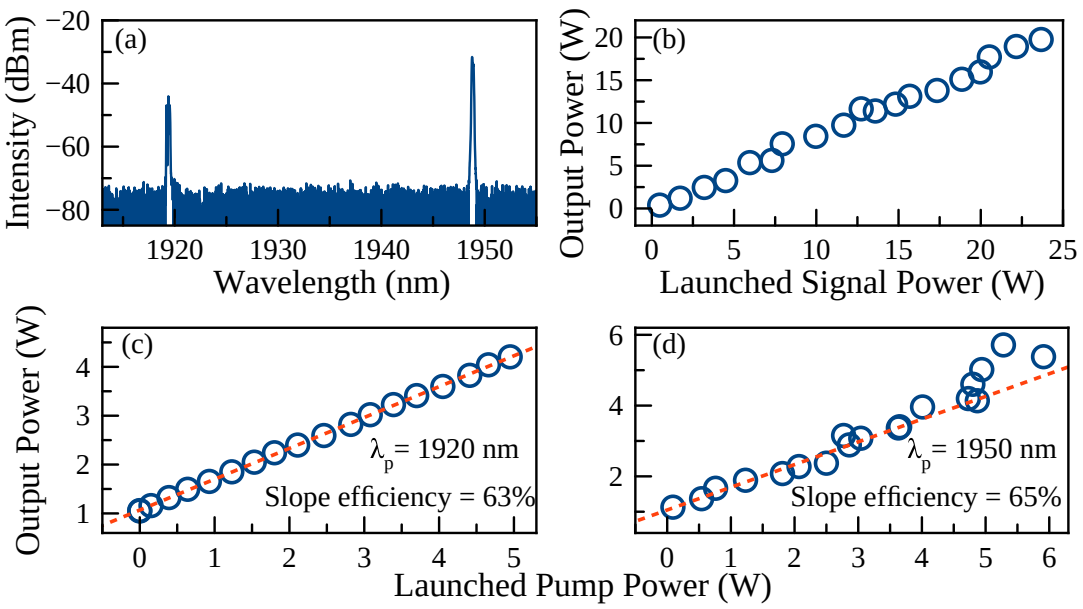

Figure 5.6: (a) Spectral measurement at the output port of WDM1 and combined optical power with respect to the launched signal power of the fiber lasers (1920 & 1950 nm). Measured output power of the Ho-doped fiber amplifier with respect to launched pump power for individual pump wavelengths (c) 1920 nm and (d) 1950 nm.

depicted in Fig 5.7(a). We achieved more than 8 W of output power at a total input power of 12 W and the linear fitted slope efficiency is calculated to be 68 %. Additionally, the temperature distribution along the Ho-doped fiber core will be measured with a high resolution pyrometer for observing the effect of dual wavelength pumping technique on the temperature distribution of the gain fiber. The difference between absoprtion cross section values of 1920 nm and 1950 nm represent the amount of pump to signal conversion from the beginning of the gain medium. The pump sources emitting 1920 nm and 1950 nm have almost same lasing efficiencies simultaneously with the optimized the length of gain fiber (see Fig. 5.6), yet the amount of generating excessive heat is still major restriction in a higher average power domain with the conventional single wavelength pumping scheme. In here we are expecting after the temperature measurement of the gain fiber by using a thermal camera that the heat dissipation issue can be effectively solved by using dual wavelength pump sources, optimizing pump absorption co-efficients and fiber lengths which is investigated through numerical modeling in

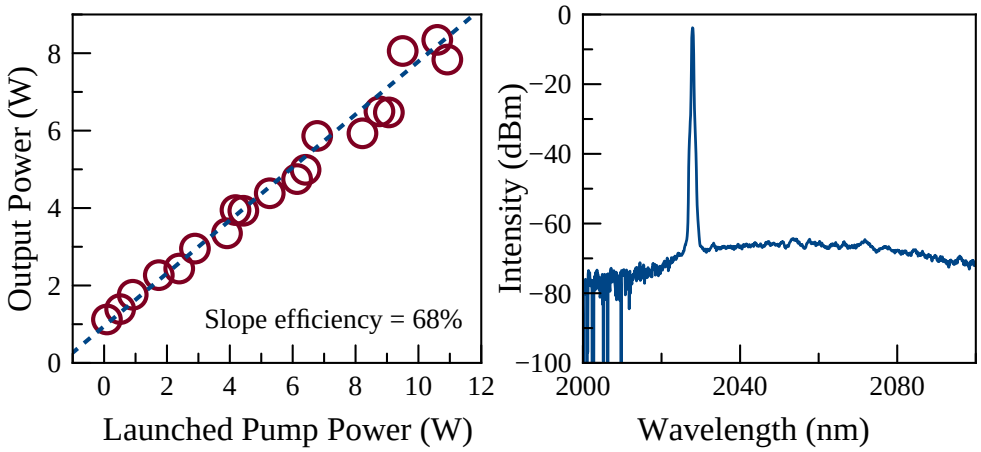

Figure 5.7: (a) Measured output power with respect to combined pump power with 68% efficiency (b) Measured optical spectrum at output power of 9 W.

the Ref. [138].

5.3.3 Conclusion

In summary, the WDM cascade design provided a solution based on all-fiber laser design and we developed the spectrally combined laser source by using a core pumping technique by using this cascade design. Additionaly, we proposed temperature management in Ho-doped fiber amplifiers by employing dual-wavelength pumping. This configuration using different pump absorption coefficients along the cavity can improve the laser efficiency and reduce temperature gradients in the fiber to some extent [138]. We obtained an average power of 9 W from Ho-doped fiber amplifier resulted in an efficiency of 68 % with the dual wavelength pumping concept. Our results can however be applied to cases with higher output power for continuous and pulsed operation. Our approach can be improved upon even with existing pump sources with different cross section values since the parameters for WDMs are available for the combination of these sources. For example, this idea can be implemented to the burst-mode amplification as investigated in Chapter 4 which could lead to reduction in the nonlinear effects while

keeping the maximum local heat generation very low.

Chapter 6

Conclusion

It is well known that the use of ultrafast (subpicosecond) pulses has potential for producing material modification or ablation on different kind of materials in the so called non-thermal, nonlinear regime, which leads to more precise and uniform material removal with small heat affected zone that cannot be achieved with traditional laser processing [140]. Therefore, high-precision material processing assisted by ultrafast laser pulses is gaining a great attention while laser sources are becoming well-developed tools for industrial applications and catching up with industry requirements. However, ultrafast pulse laser ablation suffers from the limited ablation depth and speed. Material processing efficiency of ultrafast pulses can be dramatically increased by scaling up the repetition rate of the pulses, if the conditions are chosen correctly for avoiding undesired effects like excessive plasma and particulate shielding. However, due to a minimum pulse energy requirement for reaching an ablation threshold, continuous operation at high repetition rates can be detrimental due to high average power leading to heat accumulation. In addition to the fact that the speed with which the laser beam can be repositioned over a target is limited. Burst-mode operation of lasers, wherein the amplifier periodically produces a group of pulses (a burst), which are very closely spaced in time, can be the revolutionary solution for avoiding these problems. Indeed, burst-mode material processing already has substantial benefits [45], but the possibility of ablation cooling has recently been recognized

by our group [1]. Therefore, this thesis has presented series of work with the regards to improving the performance of fiber lasers for exploiting the ablation cooled regime.

In order to benefit from ablation cooling, the repetition rate must exceed a critical value, which scales with the thermal conductivity of the target material, at least tens of MHz as an intra-burst repetition rate. The third chapter of this thesis has represented the experimental results about works of high repetition rate fiber oscillators. The fourth chapter consists of two different fiber oscillators with different mode-locking techniques. The first laser was built at 1 μm wavelength range with Yb gain medium. We preferred all-normal dispersion mode-locked Yb-doped fiber oscillator as a seed. Several distinct mode-locked regimes can be utilized such as soliton like, stretched-pulse, similariton, and all-normal dispersion. Among these, the ANDi laser does not require the use of diffraction gratings and has the potential for all fiber integration. Owing to its simplicity and robustness, we have adapted an ANDi laser as a seed source with a fundamental repetition rate of 100 MHz. The fundamental repetition rate of this oscillator was limited by the physical size of components and also an insufficient threshold power for inducing passive mode-locking mechanism. Considering the technologically important materials like silicon, the thermal relaxation times can be measured as in the range of nanosecond which corresponds to the range of GHz. Therefore, different approaches should be investigated to generate high repetition rate pulses beyond the limits of the optical cavity. Depending on this purpose, second oscillator design was built based on a different mode-locking principle which is so called dissipative four wave mixing [65] and in this design, we preferred Erbium as a gain medium and net cavity dispersion (β_{net}) was varied from normal to anomalous dispersion regimes. As a result of this, a stable pulse formation with the repetition rate of 100 GHz for all dispersion regimes obtained and the obtained results verified that the principle of the pulse formation was dominated by dissipative four wave mixing.

The burst-mode operation not only allows dramatic increases in material removal rate per unit time and power, but effectively catapults fiber lasers, generating $\sim$10-μJ energies, to the effective level (as far as material processing is

concerned) of ∼1-mJ pulses, which are routinely available from solid state lasers. Following the demonstration of the first burst-mode fiber laser [42], here, we presented results with up to 150 W of average power which was seeded with a mode-locked fiber oscillator explaining in chapter 3, with pulse durations around sub-20 ps, individual pulse energies up to 15 μJ, number of pulses within one burst adjustable between 10 and 125, corresponding to burst energies of 100 μJ to 1.9 mJ and burst repetition rates adjustable between 80 kHz and 1 MHz. Due to the lower repetition rates required for burst-mode operation, a detailed characterization of amplified spontaneous emission (ASE) generation between the bursts is essential, which is monitored here directly using a specialty setup, that can be seen in the forth chapter. To this end, a fiber-integrated acousto-optic modulator was used, gating the laser signal such that burst signal was blocked and only ASE between the bursts was transmitted. The ASE ratio as a function of the burst repetition rate was measured as a function of average power for burst repetition rate of 1 MHz. For the ASE measurements, average power was kept at 50 W and pulse energy at $\sim 5\mu$J in order not to damage the measurement setup. We find that ASE ratio remains in the range of a harmless, acceptable 2 % for burst repetition rates of 200 kHz and higher.

The fifth chapter of this thesis is devoted to develop a fiber laser amplifier system operating around 2 μm for transparent material and tissue processing applications. Our know-how on Yb-fiber laser amplifier systems operating at 1 μm which is explained in chapter 4 transferred to the fiber laser systems operating around 2 μm. However the systems operating around the wavelength range of 2 μm are newly emerged and historically lagged behind the other gain mediums like Ytterbium due to the technological developments. Therefore, the fifth chapter contains two main sections corresponding to developing core technologies for the fiber laser systems at 2 μm. First section presented the design and construction of the high brightness pump source for the amplification of Holmium at 2 μm wavelength regime, because pumping with very high brightness fiber lasers allows for the control of the core-to-clad ratio and therefore, the pump absorption per fiber length. This enables a trade-off between head load e.g., for mitigation of mode instabilities and nonlinearities by adjusting the fiber length. The spectral

beam combination provides versatile solutions to preserving the brightness of laser beams of arbitrary wavelength while scaling up the average power. Therefore, it is a key technology that must be further explored and developed. Consequently, we planned to investigate scaling the power of single Tm-doped fiber lasers and explored to spectrally combine a large array of lasers by using an in-house-made WDM cascade. We were using a custom-made WDMs cascade system for spatially combining signals and scaling up the lasers power available from a single mode fiber laser. The experimental setup contained three identical continuous wave oscillators, each emitting signals at four distinct wavelengths, which were 1920 nm, 1950 nm, 1977 nm and 2030 nm. The constituent lasers were combined by using an in-house-made WDMs. We achieved more than 38 W of output power with 69% of the combining efficiency. In the second section, we have developed resonantly core-pumped holmium fiber lasers primarily for high power laser applications in the 2 m spectral region by all-fiber truly single mode Tm-doped fiber lasers combined with WDM cascade. Despite the higher threshold for nonlinear effects at longer wavelengths, scaling the power of the Ho-doped fiber amplifier with Tm-doped fiber lasers still have limitations. Thermal effects, which limit the average power, can be minimized by using low-doped, longer gain fibers, whereas the presence of nonlinear effects requires the use of high doped, shorter fibers to maximize the average or peak power of the system. We propose the use of two different pump wavelengths with different absorption coefficient along the gain fiber as an analogy to doping management to circumvent these opposing requirements. As a practical first implementation, we report on the development of a fiber laser amplifier system which composed of Ho-doped fiber with the length of 2 meters and pumped by Tm-doped fiber lasers at the wavelengths of 1920 nm and 1950 nm. We obtained an average power of 9 W from the Ho-doped amplifier resulted in an efficiency of 68 %.

Bibliography

[1] C. Kerse, H. Kalaycıoğlu, P. Elahi, B. Çetin, D. K. Kesim, Ö. Akçaalan, S. Yavaş, M. D. Aşık, B. Öktem, H. Hoogland, R. Holzwarth and F. Ö. Ilday, "Ablation-cooled material removal with ultrafast bursts of pulses," *Nature*, vol. 4, July 2016.

[2] H. Kalaycıoğlu, K. Eken and F. Ö. Ilday, "Fiber amplification of pulse bursts up to 20 μJ pulse energy at 1 kHz repetition rate," *Optics Letters*, vol. 36, September 2011.

[3] U. Keller, K. J. Weingarten, F. X. Kartner, D. Kopf, B. Braun, I. D. Jung, R. Fluck, C. Honninger, N. Matuschek and J. A. Der Au, "Semiconductor saturable absorber mirrors (SESAM's) for femtosecond to nanosecond pulse generation in solid-state lasers," *IEEE Journal of selected topics in QUANTUM ELECTRONICS*, vol. 2, no. 3, pp. 435–453, 1996.

[4] R. Paschotta and U. Keller, "Passive mode locking with slow saturable absorbers," *Applied Physics B*, vol. 73, no. 7, pp. 653–662, 2001.

[5] T. H. Maiman, "Stimulated optical radiation in Ruby," *Nature*, vol. 187, no. 4736, pp. 493–494, 1960.

[6] U. Keller, "Recent developments in compact ultrafast lasers," *Nature*, vol. 424, no. 6950, pp. 831–838, 2003.

[7] A. Javan, W. R. Bennett Jr. and D. R. Herriott, "Population inversion and continuous optical maser oscillation in a gas discharge containing a He-Ne mixture," *Physical Review Letters*, vol. 6, no. 106, 1961.

[8] F. J. McClung and R. W. Hellwarth, "Giant optical pulsation from Ruby," *Journal of Applied Physics*, vol. 33, no. 828, 1962.

[9] H. W. Mocker and R. J. Collins, "Mode competition and self-locking effects in a Q-switched Ruby laser," *Applied Physics Letters*, vol. 7, no. 270, 1965.

[10] E. P. Ippen, C. V. Shank and A. Dienes, "Passive mode-locking of the CW dye laser," *Applied Physics Letters*, vol. 21, no. 348, 1972.

[11] C. J. Koester and E. Snitzer, "Amplification in a fiber laser," *Applied Optics*, vol. 3, pp. 1182–1186, October 1964.

[12] E. Snitzer, "Optical maser action of Nd+ 3 in a barium crown glass," *Physical Review Letters*, vol. 7, no. 12, p. 444, 1961.

[13] J. D. Barry and A. J. Einhorn, "Laser pumping system," May 1983. US Patent 4,383,318.

[14] R. J. Mears and L. Reekie and I. M. Jauncey and D. N. Payne, "Low-noise Erbium-doped fibre amplifier operating at 1.54μm," *Electronics Letters*, vol. 19, no. 23, pp. 1026–1028, 1987.

[15] E. Desurvire,J. R. Simpson and P. C. Becker, "High-gain Erbium-doped traveling-wave fiber amplifier," *Optics Letters*, vol. 12, no. 11, pp. 888–890, 1987.

[16] V. Gapontsev, V. Fomin, A. Ferin and M. Abramov, "Diffraction limited ultra-high-power fiber lasers," in *Lasers, Sources and Related Photonic Devices*, p. AWA1, Optical Society of America, 2010.

[17] T. Eidam, S. Hanf, E. Seise, T. V. Andersen, T. Gabler, C. Wirth, T. Schreiber, J. Limpert and Andreas Tünnermann, "Femtosecond fiber CPA system emitting 830 W average output power," *Optics Letters*, vol. 35, pp. 94–96, January 2010.

[18] C. Kerse, H. Kalaycıoğlu, P. Elahi, Ö. Akçaalan and F. Ö. Ilday, "3.5-GHz intra-burst repetition rate ultrafast Yb-doped fiber laser," *Optics Communications*, vol. 366, pp. 404–409, 2016.

[19] D. J. Richardson, J. Nilsson and W. A. Clarkson, "High power fiber lasers: current status and future perspectives [invited]," *JOSA B*, vol. 27, no. 11, pp. B63–B92, 2010.

[20] M. E. Fermann and I. Hartl, "Ultrafast fibre lasers," *Nature Photonics*, vol. 7, pp. 868–874, October 2013.

[21] C. Xu and F. W. Wise, "Recent advances in fibre lasers for nonlinear microscopy," *Nature Photonics*, vol. 7, pp. 875–882, October 2013.

[22] B. Shiner, "The fibre laser: Delivering power," *Nature Photonics*, vol. 4, pp. 875–882, 2010.

[23] C. Jauregui, J. Limpert and A. Tünnerman, "High-power fibre lasers," *Nature Photonics*, vol. 7, pp. 861–867, 2013.

[24] B. Öktem, I. Pavlov, S. Ilday, H. Kalaycıoğlu, A. Rybak, S. Yavaş, M. Erdoğan and F. Ö. Ilday, "Nonlinear laser lithography for indefinitely large area nanostructuring with femtosecond pulses," *Nature Photonics*, vol. 7, pp. 897–901, 2013.

[25] W. Demtröder, *Laser spectroscopy: basic concepts and instrumentation*. Springer Science & Business Media, 2013.

[26] Th. Udem, J. Reichert, R. Holzwarth and T. W. Hänsch, "Absolute optical frequency measurement of the cesium D 1 line with a mode-locked laser," *Physical Review Letters*, vol. 82, no. 18, p. 3568, 1999.

[27] G. P. Agrawal, *Nonlinear fiber optics*. Academic press, 2007.

[28] R. R. Gattass and E. Mazur, "Femtosecond laser micromachining in transparent materials," *Nature photonics*, vol. 2, no. 4, pp. 219–225, 2008.

[29] W. Yang, P. G. Kazansky and Y. P. Svirko, "Non-reciprocal ultrafast laser writing," *Nature Photonics*, vol. 2, no. 2, pp. 99–104, 2008.

[30] J. D. Steinmeyer, C. L. Gilleland, C. Pardo-Martin, M. Angel, C. B. Rohde, M. A. Scott and M. F. Yanik, "Construction of a femtosecond laser microsurgery system," *Nature protocols*, vol. 5, no. 3, pp. 395–407, 2010.

[31] A. Plech, V. Kotaidis, M. Lorenc and J. Boneberg, "Femtosecond laser near-field ablation from gold nanoparticles," *Nature Physics*, vol. 2, no. 1, pp. 44–47, 2006.

[32] A. Rousse, C. Rischel, S. Fourmaux, I. Uschmann, S. Sebban, G. Grillon, Ph. Balcou, E. Förster, J.P. Geindre P. Audebert, J. C. Gauthier and D. Hulin, "Non-thermal melting in semiconductors measured at femtosecond resolution," *Nature*, vol. 410, no. 6824, pp. 65–68, 2001.

[33] S. H. Chung and E. Mazur, "Surgical applications of femtosecond lasers," *Journal of biophotonics*, vol. 2, no. 10, pp. 557–572, 2009.

[34] J. Serbin, T. Bauer, C. Fallnich, A. Kasenbacher and W. H. Arnold, "Femtosecond lasers as novel tool in dental surgery," *applied surface science*, vol. 197, pp. 737–740, 2002.

[35] B. N. Chichkov, C. Momma, S. Nolte, F. Von Alvensleben and A. Tünnermann, "Femtosecond, picosecond and nanosecond laser ablation of solids," *Applied Physics A*, vol. 63, no. 2, pp. 109–115, 1996.

[36] F. Bauer, A. Michalowski, T. Kiedrowski and S. Nolte, "Heat accumulation in ultra-short pulsed scanning laser ablation of metals," *Optics express*, vol. 23, no. 2, pp. 1035–1043, 2015.

[37] X. Liu, D. Du and G. Mourou, "Laser ablation and micromachining with ultrashort laser pulses," *IEEE journal of quantum electronics*, vol. 33, no. 10, pp. 1706–1716, 1997.

[38] E. G. Gamaly, A. V. Rode, B. Luther-Davies and V. T. Tikhonchuk, "Ablation of solids by femtosecond lasers: Ablation mechanism and ablation thresholds for metals and dielectrics," *Physics of Plasmas (1994-present)*, vol. 9, no. 3, pp. 949–957, 2002.

[39] T. Juhasz, F. H. Loesel, R. M. Kurtz, C. Horvath, J. F. Bille and G. Mourou, "Corneal refractive surgery with femtosecond lasers," *IEEE Journal of Selected Topics in Quantum Electronics*, vol. 5, no. 4, pp. 902–910, 1999.

[40] J. Bonse, J. Krüger, S. Höhm and A. Rosenfeld, "Femtosecond laser-induced periodic surface structures," *Journal of Laser Applications*, vol. 24, no. 4, p. 042006, 2012.

[41] W. Hu, Y. C. Shin and G. King, "Modeling of multi-burst mode picosecond laser ablation for improved material removal rate," *Applied Physics A*, vol. 98, no. 2, pp. 407–415, 2010.

[42] H. Kalaycıoğlu, Y. B. Eldeniz, Ö. Akçaalan, S. Yavaş, K. Gürel, M. Efe and F. Ö. Ilday, , "1 mJ pulse bursts from a Yb-doped fiber amplifier," *Optics letters*, vol. 37, no. 13, pp. 2586–2588, 2012.

[43] S. Breitkopf, A. Klenke, T. Gottschall, H. J. Otto, C. Jauregui, J. Limpert and A. Tünnermann, "58 mJ burst comprising ultrashort pulses with homogenous energy level from an Yb-doped fiber amplifier," *Optics letters*, vol. 37, no. 24, pp. 5169–5171, 2012.

[44] M. Lapczyna, K. P. Chen, P. R. Herman, H. W. Tan and R. S. Marjoribanks, "Ultra high repetition rate (133 MHz) laser ablation of aluminum with 1.2-ps pulses," *Applied Physics A*, vol. 69, no. 1, pp. S883–S886, 1999.

[45] R. S. Marjoribanks, C. Dille, J. E. Schoenly, L. McKinney, A. Mordovanakis, P. Kaifosh, P. Forrester, Z. Qian, A. Covarrubias, Y. Feng and L. Lilge, "Ablation and thermal effects in treatment of hard and soft materials and biotissues using ultrafast-laser pulse-train bursts," *Photonics and Lasers in Medicine*, vol. 1, no. 3, pp. 155–169, 2012.

[46] Z. Qian, A. Mordovanakis, J. E. Schoenly, A. Covarrubias, Y. Feng, L. Lilge and R. S. Marjoribanks, "Pulse train-burst mode, ultrafast-laser interactions with 3D viable cell cultures as a model for soft biological tissues," *Biomedical optics express*, vol. 5, no. 1, pp. 208–222, 2014.

[47] H. Kalaycıoğlu, Ö. Akçaalan, S. Yavaş, Y. B. Eldeniz and F. Ö. Ilday, "Burst-mode Yb-doped fiber amplifier system optimized for low-repetition-rate operation," *JOSA B*, vol. 32, no. 5, pp. 900–906, 2015.

[48] S. Yılmaz, P. Elahi, H. Kalaycıoğlu and F. Ö. Ilday, "Amplified spontaneous emission in high-power burst-mode fiber lasers," *JOSA B*, vol. 32, no. 12, pp. 2462–2466, 2015.

[49] I. Harti, G. Imeshev, L. Dong, G. C. Cho and M. E. Fermann, "Ultra-compact dispersion compensated femtosecond fiber oscillators and amplifiers," in *(CLEO). Conference on Lasers and Electro-Optics, 2005.*, vol. 3, pp. 1641–1643, May 2005.

[50] E. Baumann, F. R. Giorgetta, J. W. Nicholson, W. C. Swann, I. Coddington and N. R. Newbury, "High performance, vibration-immune fiber laser freqeuncy comb," *Optics Letters*, vol. 35, pp. 638–640, 2009.

[51] K. Kieu, W. H. Renninger, A. Chong and F. W. Wise, "Sub-100 fs pulses at watt-level powers from a dissipative-soliton fiber laser," *Optics letters*, vol. 34, no. 5, pp. 593–595, 2009.

[52] E. Ilbey, I. Pavlov, E. Dulgergil, B. Öktem, S. Yavas, A. Rybak, Z. Zhang and F. O. Ilday, "Nonlinear chirped pulse amplification of a soliton similariton laser to 1 μJ at 1550 nm," in *Conference on Lasers and Electro-Optics 2012*, p. CTu2M.2, Optical Society of America, 2012.

[53] F. Morin, F. Druon, M. Hanna and P. Georges, "Microjoule femtosecond fiber laser at 1.6 μm for corneal surgery applications," *Optics letters*, vol. 34, no. 13, pp. 1991–1993, 2009.

[54] A. Ancona, F. Röser, K. Rademaker, J. Limpert, S. Nolte and A. Tünnermann, "High speed laser drilling of metals using a high repetition rate, high average power ultrafast fiber CPA system," *Optics Express*, vol. 16, no. 12, pp. 8958–8968, 2008.

[55] K. Özgören, B. Öktem, S. Yilmaz, F. Ö. Ilday and K. Eken, "83 W, 3.1 MHz, square-shaped, 1 ns-pulsed all-fiber-integrated laser for micromachining," *Optics express*, vol. 19, no. 18, pp. 17647–17652, 2011.

[56] F. Stutzki, F. Jansen, A. Liem, C. Jaurequi, J. Limpert and A. Tünnermann, "26 mJ 130 W Q switched fiber laser system with near diffraction limited beam quality," *Optics letters*, vol. 37, no. 6, pp. 1073–1075, 2012.

[57] M. E. Fermann, "Single-mode excitation of multimode fibers with ultrashort pulses," *Optics Letters*, vol. 23, no. 1, pp. 52–54, 1998.

[58] J. P. Koplow, D. A. V. Kliner and L. Goldberg, "Single-mode operation of a coiled multimode fiber amplifier," *Optics letters*, vol. 25, no. 7, pp. 442–444, 2000.

[59] X. Ma, C.H. Liu, G. Chang and A. Galvanauskas, "Angular-momentum coupled optical waves in chirally-coupled-core fibers," *Optics express*, vol. 19, no. 27, pp. 26515–26528, 2011.

[60] T. Eidam, J. Rothhardt, F. Stutzki, F. Jansen, S. Hädrich, H. Carstens, C. Jauregui, J. Limpert and Andreas Tünnermann, "Fiber chirped-pulse amplification system emitting 3.8 GW peak power," *Optics Express*, vol. 19, no. 1, pp. 255–260, 2011.

[61] R. J. Essiambre, G. Kramer, P. J. Winzer, G. J. Foschini and B. Goebel, "Capacity limits of optical fiber networks," *Journal of Lightwave Technology*, vol. 28, no. 4, pp. 662–701, 2010.

[62] D. Cotter, R. J. Manning, K. J. Blow, A. D. Ellis, A. E. Kelly, D. Nesset, I. D. Phillips, A. J. Poustie and D. C. Rogers, "Nonlinear optics for high-speed digital information processing," *Science*, vol. 286, no. 5444, pp. 1523–1528, 1999.

[63] T. Habruseva, S. O'Donoghue, N. Rebrova, F. Kefelian, S. P. Hegarty and G. Huyet, "Optical linewidth of a passively mode-locked semiconductor laser," *Optics letters*, vol. 34, no. 21, pp. 3307–3309, 2009.

[64] P. Franco, F. Fontana, I. Cristiani, M. Midrio and M. Romagnoli, "Self-induced modulational-instability laser," *Optics letters*, vol. 20, no. 19, pp. 2009–2011, 1995.

[65] M. Quiroga-Teixeiro, C. B. Clausen, M. P. Sørensen, P. L. Christiansen and P. A. Andrekson, "Passive mode locking by dissipative four-wave mixing," *JOSA B*, vol. 15, no. 4, pp. 1315–1321, 1998.

[66] R. Paschotta, J. Nilsson, A. C. Tropper and D. C. Hanna, "Ytterbium-doped fibre amplifiers," *IEEE Journal of quantum electronics*, vol. 33, no. 7, pp. 1049–1056, 1997.

[67] B. E. A. Saleh, M. C. Teichl and B. E. Saleh, *Fundamentals of photonics*, vol. 22. Wiley New York, 1991.

[68] C. R. Giles and E. Desurvirel, "Modeling Erbium-doped fiber amplifiers," *Journal of lightwave technology*, vol. 9, no. 2, pp. 271–283, 1991.

[69] B. J. Ainslie, "A review of the fabrication and properties of Erbium-doped fibers for optical amplifiers," *Journal of Lightwave Technology*, vol. 9, no. 2, pp. 220–227, 1991.

[70] P. F. Moulton,G. A. Rines, E. V. Slobodtchikov, K. F. Wall, G. Frith, B. Samson and A. L. G. Carter, "Tm-doped fiber lasers: fundamentals and power scaling," *IEEE Journal of Selected Topics in Quantum Electronics*, vol. 15, no. 1, pp. 85–92, 2009.

[71] J. A. Buck, *Fundamentals of optical fibers*. John Wiley & Sons, 2004.

[72] M. Courtney, N. Spellmeyer, H. Jiao and D. Kleppner, "Classical, semiclassical, and quantum dynamics in the lithium Stark system," *Physical Review A*, vol. 51, no. 5, p. 3604, 1995.

[73] J. Xu, M. Prabhu, J. Lu, K. I. Ueda and D. Xing, "Efficient double-clad Thulium-doped fiber laser with a ring cavity," *Applied optics*, vol. 40, no. 12, pp. 1983–1988, 2001.

[74] R. W. Boyd, *Nonlinear optics*. Academic press, 2003.

[75] N. Akhmediev and A. Ankiewicz, "Dissipative solitons in the complex Ginzburg-Landau and Swift-Hohenberg equations," in *Dissipative Solitons*, pp. 1–17, Springer, 2005.

[76] A. Chong, J. Buckley, W. Renninger and F. Wise, "All-normal-dispersion femtosecond fiber laser," *Optics Express*, vol. 14, no. 21, pp. 10095–10100, 2006.

[77] D. Kuizenga and A. Siegman, "FM and AM mode locking of the homogeneous laser-Part i: Theory," *IEEE Journal of Quantum Electronics*, vol. 6, no. 11, pp. 694–708, 1970.

[78] H. A. Haus, "Mode-locking of lasers," *IEEE Journal of Selected Topics in Quantum Electronics*, vol. 6, no. 6, pp. 1173–1185, 2000.

[79] F. X. Kurtner, J. A. der Au, and U. Keller, "Mode-locking with slow and fast saturable absorbers-what's the difference?," *IEEE Journal of Selected Topics in Quantum Electronics*, vol. 4, no. 2, pp. 159–168, 1998.

[80] H. A. Haus, A. Hermann, J. G. Fujimoto and E. P. Ippen, "Structures for additive pulse mode locking," *JOSA B*, vol. 8, no. 10, pp. 2068–2076, 1991.

[81] H. A. Haus, "Theory of mode locking with a fast saturable absorber," *Journal of Applied Physics*, vol. 46, no. 7, pp. 3049–3058, 1975.

[82] E. G. Gamaly and A. V. Rode, "Physics of ultra-short laser interaction with matter: From phonon excitation to ultimate transformations," *Progress in Quantum Electronics*, vol. 37, no. 5, pp. 215–323, 2013.

[83] M. Mangold, C. A. Zaugg, S. M. Link, M. Golling, B. W. Tilma and U. Keller, "Pulse repetition rate scaling from 5 to 100 GHz with a high-power semiconductor disk laser," *Optics express*, vol. 22, no. 5, pp. 6099–6107, 2014.

[84] C. Li, Y. Ma, X. Gao, F. Niu, T. Jiang, A. Wang and Z. Zhang, "1 GHz repetition rate femtosecond Yb: fiber laser for direct generation of carrier-envelope offset frequency," *Applied optics*, vol. 54, no. 28, pp. 8350–8353, 2015.

[85] J. Chen, J. W. Sickler, P. Fendel, E. P. Ippen, F. X. Kärtner, T. Wilken, R. Holzwarth and T. W. Hänsch, "Generation of low-timing-jitter femtosecond pulse trains with 2 GHz repetition rate via external repetition rate multiplication," *Optics letters*, vol. 33, no. 9, pp. 959–961, 2008.

[86] R. Eason, *Pulsed laser deposition of thin films: applications-led growth of functional materials*. John Wiley & Sons, 2007.

[87] N. G. Horton, K. Wang, D. Kobat, C. G. Clark, F. W. Wise, C. B. Schaffer and C. Xu, "In vivo three-photon microscopy of subcortical structures within an intact mouse brain," *Nature photonics*, vol. 7, no. 3, pp. 205–209, 2013.

[88] S. W. Smye, J. M. Chamberlain, A. J. Fitzgerald and E. Berry, "The interaction between terahertz radiation and biological tissue," *Physics in medicine and biology*, vol. 46, no. 9, p. R101, 2001.

[89] R. Kammel, R. Ackermann, J. Thomas, J. Götte, S. Skupin, A. Tünnermann and S. Nolte, "Enhancing precision in fs-laser material processing by simultaneous spatial and temporal focusing," *Light: Science & Applications*, vol. 3, no. 5, p. e169, 2014.

[90] P. Elahi, S. Yılmaz, Ö. Akçaalan, H. Kalaycıoğlu, B. Öktem, CÇ. Senel and F. Ö. Ilday and K. Eken, "Doping management for high-power fiber lasers: 100 W, few-picosecond pulse generation from an all-fiber-integrated amplifier," *Optics letters*, vol. 37, no. 15, pp. 3042–3044, 2012.

[91] L. E. Nelson, D. J. Jones, K. Tamura, H. A. Haus and E. P. Ippen, "Ultrashort-pulse fiber ring lasers," *Applied Physics B: Lasers and Optics*, vol. 65, no. 2, pp. 277–294, 1997.

[92] F. Ö. Ilday, H. Lim, J. R. Buckley, and F. W. Wise, "Practical all-fiber source of high power 120-fs pulses at 1 μm," *Optics Letters*, vol. 28, no. 15, 2003.

[93] P. K. Mukhopadhyay, K. Özgören, I. L. Budunoglu, and F. Ö. Ilday, "All-fiber low noise high-power femtosecond Yb fiber amplifier system seeded by

an all normal dispersion fiber oscillator," *IEEE Journal of Selected Topics in Quantum Electronics*, vol. 15, no. 1, 2009.

[94] E. Yoshida and M. Nakazawa, "Low-threshold 115-GHz continuous-wave modulational-instability erbium-doped fiber laser," *Optics letters*, vol. 22, no. 18, pp. 1409–1411, 1997.

[95] T. Sylvestre, S. Coen, P. Emplit and M. Haelterman, "Self-induced modulational instability laser revisited: normal dispersion and dark-pulse train generation," *Optics letters*, vol. 27, no. 7, pp. 482–484, 2002.

[96] M. Peccianti, A. Pasquazi, Y. Park, B. E. Little, S. T. Chu, D. J. Moss and R. Morandotti, "Demonstration of a stable ultrafast laser based on a nonlinear microcavity," *Nature communications*, vol. 3, p. 765, 2012.

[97] P. A. Bélanger, L. Gagnon and C. Paré, "Solitary pulses in an amplified nonlinear dispersive medium," *Optics letters*, vol. 14, no. 17, pp. 943–945, 1989.

[98] V. S. Grigoryan, A. I. Maimistov and Y. M. Skylarov, "Evolution of light pulses in a nonlinear amplifying medium," *Journal of Experimental and Theoretical Physics*, vol. 67, no. 3, pp. 530–534, 1988.

[99] M. Quiroga-Teixeiro, C. B. Clausen, M. P. Sørensen, P. L. Christiansen and P. A. Andrekson, "Passive mode locking by dissipative four-wave mixing," *JOSA B*, vol. 15, no. 4, pp. 1315–1321, 1998.

[100] J. Schröder, T. D. Vo and B. J. Eggleton, "Repetition-rate-selective, wavelength-tunable mode-locked laser at up to 640 GHz," *Optics letters*, vol. 34, no. 24, pp. 3902–3904, 2009.

[101] C. Kerse, S. Yavaş, H. Kalaycıoğlu, M. D. Aşık, Ö. Akçaalan and F. Ö. Ilday, "High-speed, thermal damage-free ablation of brain tissue with femtosecond pulse bursts," in *Conference on Lasers and Electro-Optics/Pacific Rim*, p. 25H3_3, Optical Society of America, 2015.

[102] C. Kerse, S. Yavaş, H. Kalaycıoğlu, M. D. Aşık, Ö. Akçaalan and F. Ö. Ilday, "Efficient, high-speed ablation of soft tissue with few-microjoule, femtosecond pulse bursts," *arXiv preprint arXiv:1410.6730*, 2014.

[103] K. Sugioka and Y. Cheng, *Ultrafast laser processing: from micro to nanoscale*. CRC Press, 2013.

[104] R. Srinivasan and B. Braren, "Ultraviolet laser ablation of organic polymers," *Chemical Reviews*, vol. 89, no. 6, pp. 1303–1316, 1989.

[105] M. Lenzner, J. Krüger, W. Kautek and F. Krausz, "Precision laser ablation of dielectrics in the 10-fs regime," *Applied Physics A: Materials Science & Processing*, vol. 68, no. 3, pp. 369–371, 1999.

[106] C. Momma, B. N. Chichkov, S. Nolte, F. von Alvensleben, A. Tünnermann, H. Welling and B. Wellegehausen, "Short-pulse laser ablation of solid targets," *Optics communications*, vol. 129, no. 1, pp. 134–142, 1996.

[107] P. P. Wu, W. L. Lempert and R. B. Miles, "Megahertz pulse-burst laser and visualization of shock-wave/boundary-layer interaction," *AIAA journal*, vol. 38, no. 4, pp. 672–679, 2000.

[108] P. P. Wu and R. B. Miles, "High-energy pulse-burst laser system for megahertz-rate flow visualization," *Optics Letters*, vol. 25, no. 22, pp. 1639–1641, 2000.

[109] N. Jiang, M. C. Webster and W. R. Lempert, "Advances in generation of high-repetition-rate burst mode laser output," *Applied Optics*, vol. 48, no. 4, pp. B23–B31, 2009.

[110] B. S. Thurow, A. Satija and K. Lynch, "Third-generation megahertz-rate pulse burst laser system," *Applied optics*, vol. 48, no. 11, pp. 2086–2093, 2009.

[111] D. M. Baney, P. Gallion and R. S. Tucker, "Theory and measurement techniques for the noise figure of optical amplifiers," *Optical fiber technology*, vol. 6, no. 2, pp. 122–154, 2000.

[112] P. Elahi, S. Yılmaz, Y. B. Eldeniz and F. Ö. Ilday, "Generation of picosecond pulses directly from a 100 W, burst-mode, doping-managed yb-doped fiber amplifier," *Optics letters*, vol. 39, no. 2, pp. 236–239, 2014.

[113] I. Pavlov, E. Dülgergil, E. Ilbey and F. Ö. Ilday, "Diffraction-limited, 10-W, 5-ns, 100-kHz, all-fiber laser at 1.55 μm," *Optics letters*, vol. 39, no. 9, pp. 2695–2698, 2014.

[114] J. W. Nicholson, J. Jasapara, W. Rudolph, F. G. Omenetto and A. J. Taylor, "Full-field characterization of femtosecond pulses by spectrum and cross-correlation measurements," *Optics letters*, vol. 24, no. 23, pp. 1774–1776, 1999.

[115] F. Zhang, Q. Shao, T. R. W. Herrmann, Y. Tian and Y. Zhang, "Thulium laser versus Holmium laser transurethral enucleation of the prostate: 18-month follow-up data of a single center," *Urology*, vol. 79, no. 4, pp. 869–874, 2012.

[116] J. S. Lam, T. D. Greene and M. Gupta, "Treatment of proximal ureteral calculi: Holmium: YAG laser ureterolithotripsy versus extracorporeal shock wave lithotripsy," *The Journal of urology*, vol. 167, no. 5, pp. 1972–1976, 2002.

[117] S. D. Jackson, "Cross relaxation and energy transfer upconversion processes relevant to the functioning of 2 μm Tm 3+-doped silica fibre lasers," *Optics Communications*, vol. 230, no. 1, pp. 197–203, 2004.

[118] S. Yilmaz, C. Ottenhues, T. Theeg, S. Lamrini, K. Scholle, M. Schäfer, P. Fuhrberg, H. Sayinc, F. Ö. Ilday, J. Neumann and D. Kracht, "Single-mode spectral beam combining of high power Tm-doped fiber lasers with WDM cascades," in *SPIE LASE*, pp. 97280O–97280O, International Society for Optics and Photonics, 2016.

[119] N. M. Fried and K. E. Murray, "High-power Thulium fiber laser ablation of urinary tissues at 1.94 um," *Journal of endourology*, vol. 19, no. 1, pp. 25–31, 2005.

[120] T. Bach, T. R. W. Herrmann, C. Cellarius and A. J. Gross, "Bladder neck incision using a 70 W 2 micron continuous wave laser (revolix)," *World journal of urology*, vol. 25, no. 3, pp. 263–267, 2007.

[121] C. R. Phillips, J. Jiang, C. Langrock, M. M. Fejer and M. E. Fermann, "Self-referenced frequency comb from a Tm-fiber amplifier via PPLN waveguide supercontinuum generation," in *CLEO: Applications and Technology*, p. PDPA5, Optical Society of America, 2011.

[122] S. D. Jackson, "Towards high-power mid-infrared emission from a fibre laser," *Nature photonics*, vol. 6, no. 7, pp. 423–431, 2012.

[123] A. Hemming, S. Bennetts, N. Simakov, J. Haub and A. Carter, "Development of resonantly cladding-pumped Holmium-doped fibre lasers," in *SPIE LASE*, pp. 82371J–82371J, International Society for Optics and Photonics, 2012.

[124] J. Li, D. D. Hudson and S. D. Jackson, "High-power diode-pumped fiber laser operating at 3 μm," *Optics letters*, vol. 36, no. 18, pp. 3642–3644, 2011.

[125] C. Carbonnier, H. Tobben and U. B. Unrau, "Room temperature CW fibre laser at 3.22 μm," *Electronics Letters*, vol. 34, no. 9, pp. 893–894, 1998.

[126] J. Schneide, C. Carbonnier and U. B. Unrau, "Characterization of a Ho 3+-doped fluoride fiber laser with a 3.9-μm emission wavelength," *Applied optics*, vol. 36, no. 33, pp. 8595–8600, 1997.

[127] T. Ehrenreich, R. Leveille, I. Majid, K. Tankala, G. Rines and P. Moulton, "1-kW, all-glass tm: fiber laser," in *Proc. SPIE*, vol. 7580, p. 758016, 2010.

[128] C. Wirth, O. Schmidt, I. Tsybin, T. Schreiber, R. Eberhardt, J. Limpert, A. Tünnermann, K. Ludewigt, M. Gowin, E. Ten Have and M. Yung, "High average power spectral beam combining of four fiber amplifiers to 8.2 kW," *Optics letters*, vol. 36, no. 16, pp. 3118–3120, 2011.

[129] O. Shneider, B. Shulga and A. A. Ishaaya, "Imposing narrow spectral bandwidth in a system of passively combined fiber lasers," *Optics letters*, vol. 38, no. 5, pp. 603–605, 2013.

[130] A. Hemming, N. Simakov, A. Davidson, S. Bennetts, M. Hughes, N. Carmody, P. Davies, L. Corena, D. Stepanov, J. Haub and M. Yung, "A monolithic cladding pumped holmium-doped fibre laser," in *CLEO: Science and Innovations*, pp. CW1M–1, Optical Society of America, 2013.

[131] C. Ottenhues, T. Theeg, K. Hausmann, M. Wysmolek, H. Sayinc, J. Neumann and D. Kracht, "Single-mode monolithic fiber laser with 200 W output power at a wavelength of 1018 nm," *Optics letters*, vol. 40, no. 21, pp. 4851–4854, 2015.

[132] T. Theeg, C. Ottenhues, H. Sayinc, J. Neumann and D. Kracht, "Core-pumped single-frequency fiber amplifier with an output power of 158 W," *Optics letters*, vol. 41, no. 1, pp. 9–12, 2016.

[133] G. Pelegrina-Bonilla, K. Hausmann, K. Liu, H. Sayinc, U. Morgner, J. Neumann and D. Kracht, "Matching of the propagation constants in an asymmetric single-mode fused fiber coupler for core pumping Thulium-doped fiber at 795 nm," *Optics letters*, vol. 37, no. 11, pp. 1844–1846, 2012.

[134] G. Pelegrina-Bonilla, K. Hausmann, H. Tünnermann, P. Weßels, H. Sayinc, U. Morgner, J. Neumann and D. Kracht, "Analysis of the coupling mechanism in asymmetric fused fiber couplers," *Journal of Lightwave Technology*, vol. 32, no. 13, pp. 2382–2391, 2014.

[135] T. A. Birks and Y. W. Li, "The shape of fiber tapers," *Journal of Lightwave Technology*, vol. 10, no. 4, pp. 432–438, 1992.

[136] I. Dajani, C. Zeringue and T. M. Shay, "Investigation of nonlinear effects in multitone-driven narrow-linewidth high-power amplifiers," *IEEE journal of selected topics in quantum electronics*, vol. 15, no. 2, pp. 406–414, 2009.

[137] A. Hemming, N. Simakov, J. Haub and A. Carter, "A review of recent progress in Holmium-doped silica fibre sources," *Optical Fiber Technology*, vol. 20, no. 6, pp. 621–630, 2014.

[138] Y. Wang, "Heat dissipation in kilowatt fiber power amplifiers," *IEEE journal of quantum electronics*, vol. 40, no. 6, pp. 731–740, 2004.

[139] N. Simakov, A. Hemming, A. Carter, K. Farley, A. Davidson, N. Carmody, J. M. O. Daniel, M. Hughes, L. Corena, D. Stepanov and J. Haub, "170 W single-mode large pedestal Thulium-doped fibre laser," in *The European Conference on Lasers and Electro-Optics*, p. CJ_13_2, Optical Society of America, 2015.

[140] T. Y. Choi and C. P. Grigoropoulos, "Plasma and ablation dynamics in ultrafast laser processing of crystalline silicon," *Journal of applied physics*, vol. 92, no. 9, pp. 4918–4925, 2002.

Appendix A

Code

The following code is a simple model for a mode-locked laser. This model adds up the electric field modes of a cavity (note cavity parameters can be set in the declaration section of the code), and computes the total intensity pattern. The mode-locking process is modeled by adding a phase term to each cavity mode. The user can choose to have an arbitrary amount of phase noise (set by the factor parameter) between comb components. A factor equal to 0 yields a perfect comb structure, while a factor $\geq 2\ \Pi$ yields random intensity fluctuations.

```
Em = 1; % Electric field amplitude factor
factor = 0; % noise factor (0 = phase locked, >> 0 large phase noise)
c = 3e8; % speed of light
L = 1.5; % cavity length
FSR = c/(2*L); % free spectral range of the cavity
t = -1e-9:1e-12:27e-9; % go from -1 ns to +27 ns in steps of 1 ps.
total = 0;
Upper = 1.9355e14+80*FSR; % Upper frequency limit:
% c/lambda + % (80 comb modes * FSR)

for f = 1.9355e14:FSR:Upper % go from fundamental laser frequency to
                            % higher freqs by steps of 1 FSR
```

```
phase = rand*factor; % calculate the phase for the mth mode
E = Em*cos(2*pi*f*t+phase); % calculate electric field for mth mode
total = total+E;
end
time = t./(1e-9);
plot(time,abs(total).^2/max(abs(total).^2))
xlim([-1 22])
```